UPPSALA
UNIVERSITET

UPTEC W 22002
Examensarbete 30 hp
Mars 2022

The influence of spatial variations in rain intensity for cloudburst modelling

- a case study of the Gävle cloudburst

Fanny Jeppsson Stahl

Civilingenjörsprogrammet i miljö- och vattenteknik

ABSTRACT

The influence of spatial variations in rain intensity for cloudburst modelling - a case study of the Gävle cloudburst
Fanny Jeppsson Stahl

With an intensification of heavy rain events in a changing climate and a rapid urbanization the risk for pluvial flooding is increasing in our societies. Pluvial flooding, which is formed when the rainfall rate exceeds the infiltration or drainage rate, can occur rapidly and cause great damages, large economic losses and possibly risk human lives. This kind of flooding is difficult to predict since it is caused by short-term and often local processes, but preventive measures and more robust infrastructure developed over the last decades have decreased the risk of the most severe damages. One way to prevent damage is to map risk areas and take measures by performing a cloudburst modelling, which can be done as a 2D hydraulic modelling. Common practice in cloudburst modelling today is to use a uniform design storm, often the Chicago Design Storm (CDS), with the same hyetograph applied evenly over the whole model area. Even though rain is not spatially uniform this assumption might be valid for more stratiform frontal rain. Intense rain events however have a higher spatial variation in rain intensity, and an assumption like this might significantly affect the results.

This study aimed to investigate the effect of the spatial variation in rain intensity on the modelled hydraulic response from an intense rain event. It was performed through a case study of the cloudburst in Gävle, Sweden, in August 2021. A 2D hydraulic model of the city was prepared in the software MIKE 21 Flow Model FM and the cloudburst event was simulated with a spatially varied rainfall input, based on radar data from the event with a 2×2 km resolution, and with spatially uniform rainfall input both with the temporal variation in rain intensity from the event and with a Chicago Design Storm, all with the same total volume. The scenarios were evaluated in terms of proportion of the model area being flooded, the average maximum flooding depth and by mapping the difference in flooding depth over the whole area. The results showed that the spatial variation of rainfall input had a significant effect on the hydraulic response in the city and that assuming a uniform rainfall might lead to an underestimation of the flooding depths in parts of the model area compared to a varied one. The average flooding depth was only a few percent higher for the spatially varied rain compared to the uniform rain with a similar time variation, but in large central areas of the city the model with the uniform rain underestimated the maximum flooding depth by 5-35%. The uniform CDS rain was seen to both over- and underestimate the flooding depth, but in the central and flooded parts of the city underestimation dominated. This points out a risk of using uniform design storms in cloudburst modelling, since a spatially varied rain of the same volume could give more severe effects than the simulated response and that using a uniform design storm potentially introduces an uncertainty in the modelled results that could be important to point out and further quantify.

Key words: Flood modelling, pluvial flooding, spatial variations in rain intensity, design storms, MIKE 21 Flow Model FM, 2d hydraulic modelling

Department of Earth Sciences, Program for Air, Water and Landscape Science, Uppsala University, Villavägen 16, SE-75236 Uppsala, Sweden.

REFERAT

Effekten av spatiala variationer i regnintensitet inom skyfallsmodellering - en fallstudie av Gävleskyfallet
Fanny Jeppsson Stahl

Med en intensifiering av häftiga regnväder i ett förändrat klimat och en allt snabbare urbanisering ökar risken för pluviala översvämningar i våra samhällen. Pluviala översvämningar, som skapas av att regnintensiteten är högre än infiltrations- eller dräneringshastigheten, kan uppstå plötsligt och orsaka stora skador, ekonomiska förluster och även i värsta fall riskera människoliv. Denna typ av översvämning är svår att förutse eftersom den orsakas av snabba och ofta lokala processer, men förebyggande åtgärder och mer robust infrastruktur som har utvecklats de senaste decennierna har minskat risken för de allvarligaste skadorna. Ett sätt att förebygga skador är att kartera riskområden genom skyfallsmodellering, till exempel med en tvådimensionell hydraulisk modell. Praxis idag är att använda spatialt uniforma typregn vid skyfallsmodellering, där samma hyetograf appliceras jämnt över hela modellområdet. Detta antagande kan ge giltiga resultat för mer stratiforma frontregn, men intensiva regn, skyfall, har generellt sett en hög spatial variation i intensiteten vilket gör att antagandet skulle kunna påverka resultatet signifikant.

Denna studie syftade till att undersöka effekten av den spatiala variationen i regnintensitet på den simulerade hydrauliska responsen från ett intensivt regn och den utfördes som en fallstudie av skyfallet i Gävle 17-18 augusti 2021. En 2D hydraulisk modell av Gävle förbereddes i programmet MIKE 21 Flow Model FM och simuleringar utfördes med en spatialt varierad regnindata, baserad på radardata från tillfället med en 2×2 km upplösning, och med spatialt uniforma regnindata både med den verkliga tidsvariationen och med en Chicago Design Storm (CDS), alla med samma totala volym. Skillnaden mellan scenarierna utvärderades genom att jämföra andel översvämmat modellområde, medel av maximala översvämningsdjupet och en kartering av skillnaden i översvämningsdjup över hela modellområdet. Resultaten visade att den spatiala variationen i regnindatan hade en signifikant effekt på den simulerade hydrauliska responsen i staden och att antagande om uniform regnintensitet kan leda till en underskattning av översvämningsdjupen i modellområdet jämfört med ett varierat regn. Medelvärdet av översvämningsdjupet var endast några procent högre för det spatialt varierade regnet, men i stora centrala områden underskattade modellen med det uniforma regnet det maximala översvämningsdjupet med 5-35 %. Det uniforma CDS-regnet både under- och överskattade översvämningsdjupet, men i centrala och översvämmade områden var det större delar som underskattades. Detta visar på en risk med att använda uniforma typregn i skyfallsmodellering, då ett spatialt varierat regn med samma volym skulle kunna ge betydligt allvarligare effekter än de som modellen har visat och att användandet av uniforma testregn potentiellt inför en osäkerhet i resultaten som är viktig att poängtera och även att vidare undersöka och kvantifiera.

Nyckelord: Skyfallsmodellering, pluviala översvämningar, spatiala variationer i regnintensitet, typregn, MIKE 21 Flow Model FM

Institutionen för geovetenskaper, Luft- vatten- och landskapslära, Uppsala universitet, Villavägen 16, 75236 Uppsala, Sverige.

PREFACE

With this degree project of 30 hp I am finalising my studies at the Master's Programme in Environmental and Water Engineering at Uppsala University and the Swedish University of Agricultural Sciences. The project have been carried out at Tyréns Uppsala, under supervision of Johan Kjellin and with Gabriele Messori at the Department of Earth Sciences as a subject reader.

When I finished my work for this summer, 17th of August, I went home by bus in a heavy downpour. Next morning I woke up to the news of Gävle under water and few weeks later I had a new title for my degree project. I think cloudburst is a great word, but maybe I like it even better in Swedish, 'Skyfall', simple and comprehensible but with a dramatic tone in it. I have enjoyed spending the last months diving deeper into this.

I would like to direct a huge thanks to everyone who have been involved and helped and supported me throughout the project. Thanks to Johan Kjellin for all discussions and engagement in the project. Thanks to Gabriele Messori for support, quick answers and insightful thoughts. Thanks to Max Stefansson at Tyréns who have introduced my to the modelling program and been a support all through the project and the whole Tyréns Uppsala office whom have made me feel very welcome. Thanks to Jonas Olsson at SMHI for providing me with radar data from the rain event and for interesting discussions. Thanks also to inhabitants of Gävle and photographers who have generously shared photos and experiences from the flooding. Finally but not least, a great thanks to my classmates and friends who have made this time in Uppsala a great adventure.

UPTEC W 22002 ISSN 1401-5765.
Published digitally at the Department of Earth Sciences, Uppsala University,
Uppsala, 2022.

POPULÄRVETENSKAPIG SAMMANFATTNING

Storm, skyfall och annat oväder. Vår framtid bjuder på många utmaningar i form av ett klimat som ger oss väderhändelser vilka för oss kommer te sig som extrema. Men vad som definieras som extremt beror på hur vanligt förekommande det är, och väder som klassas som extrema idag kommer i framtiden bli allt mer normala. Detta är tendenserna som IPCC har sett i flera år, och som de nu med större säkerhet än tidigare pekar ut i sin rapport som släpptes 2021. Vädret blir extremare och vad innebär då det i praktiken? Jo, till exempel beräknas skyfall öka i intensitet med ca 7 % per grads uppvärmning av medeltemperaturen och de kommer förekomma oftare. I kombination med detta har vi även en ständigt pågående urbanisering som ökar andelen hårdgjorda ytor och utökar bebyggelsen även till mindre lämpliga plaser med högre översvämningsrisk. Att förbereda våra städer för regn med så hög intensitet att de kan orsaka översvämningar är därför högeligen relevant. Med rätt förberedelser kan vi som samhälle förebygga de allvarligaste effekterna av ett skyfall, genom att planera byggandet och kanske framför allt placera samhällsviktig verksamhet så att den inte hotas av översvämning om regnet tar i lite. För att kunna ta till förebyggande åtgärder behöver vi en uppfattning om vilka områden som riskerar att översvämmas vid ett skyfall, och där är skyfallsmodellering och kartering av riskområden ett viktigt verktyg.

Idag är det praxis att skyfallskarteringar görs med rumsligt uniforma regn, regn som alltså antas ha exakt samma intensitet över hela modellområdet. Detta är en uppenbar förenkling eftersom regn förstås varierar över ett område om än i olika hög utsträckning, men det är kanske särskilt förenklande när det gäller intensiva regn som enligt många studier visar på en större variation i rummet än mer lågintensiva regn. Att undersöka hur den rumsliga variationen i regnintensitet påverkar resultatet vid en skyfallsmodellering är därför relevant och har i denna studie gjorts genom att studera skyfallet i Gävle 17-18 augusti 2021. Detta har gjorts i en skyfallsmodell som tar hänsyn till flöden, infiltration, friktion från underlaget och förstås kan hantera regnindata som varierar i både tid och rum.

Översvämningsdjup och utbredning från det rumsligt varierade regnet, baserat på radardata från tillfället, jämfördes med det från uniforma regn med samma totala volym. Typregn som används i skyfallsmodeller brukar, förutom att vara rumsligt helt uniforma, oftast ha en karaktäristisk tidsmässig variation, som kallas Chicago Design Storm (CDS). Detta är en tidsmässig variation i regnintensitet som gör att en stor del av regnet faller under en relativt kort tid, vilket riskerar att ge en överdriven översvämning jämfört med en verklig tidsvariation. Både tidsvariationen från det verkliga skyfallet och CDS-tidsvariationen användes i de uniforma regn som det rumsligt varierade jämfördes med.

Resultaten i denna studie visade att den rumsliga variationen i regnintensitet kan ha en betydande effekt på resultaten, och i vissa delar av modellområdet gav det uniforma regnet en ordentlig underskattning av översvämningsdjupet jämfört med det varierade regnet. Sett över hela området gav det rumsligt varierade regnet ett medelvärde på översvämningsdjupet som var några procent högre än de uniforma regnen, men sett till specifika delområden som drabbades av den intensivaste delen av regnet fanns det större skillnader i översvämningsdjup. Detta betyder att även om det i Gävle hade gjorts en skyfallskartering för ett regn med lika stor volym som skyfallet i augusti hade översvämningsdjupet i betydande delar av staden förmodligen underskattats, och att resultat från uniforma sky-

fallsmodelleringar potentiellt då har en betydande osäkerhet. Vi vet inte exakt hur den rumsliga variationen av ett eventuellt framtida skyfall kommer se ut, men vi kan anta att det inte är uniformt. Resultaten tyder på att vi i framtida skyfallsmodelleringar kan behöva ta större hänsyn till potentiella osäkerheter vid modellering med uniforma typregn, och dessa osäkerheter behöver undersökas vidare och kvantifieras.

Contents

1 INTRODUCTION **1**
1.1 Aims and purpose 2

2 THEORY **2**
2.1 Precipitation: formation and types 2
2.2 Extreme weather and heavy rainfall in a changing climate 4
2.3 Flooding 5
2.3.1 Pluvial flooding events in Sweden 5
2.4 Design storms and cloudburst modeling 6
2.4.1 Recommendations for cloudburst mapping 7
2.4.2 Design storms 7
2.4.3 The Chicago Design Storm 7
2.5 Spatial variation of intense rains and it's effect on modelled results 8
2.6 Hydrodynamic modeling in MIKE 21 Flow Model FM 10
2.6.1 Domain and time 10
2.6.2 Infiltration and bed resistance 10
2.6.3 Sources, precipitation and other model selections 11

3 MATERIALS AND METHODS **12**
3.1 Study site and model area 12
3.2 Model setup 13
3.2.1 Domain and mesh 13
3.2.2 Simulation time and solution technique 14
3.2.3 Other choices and input parameters 14
3.2.4 Sources 15
3.3 Precipitation input 16
3.3.1 Mean field bias adjustment of radar data 16
3.3.2 Correction of the radar data from Gävle 17
3.3.3 Preparing precipitation input to the model 18
3.4 Evaluation of scenarios 21

4 RESULTS **23**
4.1 Flooding from spatially varied rain event 23
4.1.1 Validation 23
4.2 Flooding statistics for different rain scenarios 25
4.3 Uniform with spatial mean hyetograph 26
4.4 Uniform with CDS hyetograph 31

5 DISCUSSION **35**
5.1 Precipitation input 35
5.1.1 Calibration of radar data 35
5.1.2 Deduction made for the stormwater system 36
5.1.3 The spatial resolution of the radar data 36
5.2 Other model inputs 37
5.3 Validation of the model results 38
5.4 The influence of spatial variation on the hydraulic response 39
5.5 The influence of using CDS temporal variation on the hydraulic response 41

6 CONCLUSIONS **43**

REFERENCES **45**

A APPENDIX **49**
A.1 Correction of radar estimated data against measured data 49
A.2 Flooding statistics for the full model and the central area 50
A.3 Maximum flooding depth for uniform scenarios 51
A.4 Flooding depth difference in cm for uniform scenarios 53

1 INTRODUCTION

Extreme precipitation events, or events counted as extreme today, will become increasingly frequent in a changing climate and societies need to adapt and handle the effect of these (IPCC 2021). Heavy precipitation events are particularly hazardous, as they often are associated with floods and landslides. Globally an average of 5400 persons die every year in flooding events, and large damages are made on infrastructure, cultural heritage, environment and on water quality (MSB 2012). However, deaths caused by natural disasters have generally seen a sharp decline with better ways to predict both weather and disasters, and with a more robust infrastructure (Ritchie & Roser 2014). Sweden is relatively spared when it comes to natural disasters in general and deaths are unusual in Swedish flooding events. But floods do now occur more frequently and the economic, environmental and cultural losses related to these can be rather large. The heavy precipitation is according to the IPCC (2021) very likely to become more frequent and intensify with an increasing global temperature and the intensity of extreme daily precipitation events is with high confidence estimated to increase by 7% for every degree of global warming. Therefore it is of a high importance to investigate were flooding would occur after a cloudburst and take measures to prevent possibly dangerous effects and high societal costs.

Cloudburst modelling and mapping of risk areas is one way to predict the effect of a heavy rainfall in an area and enable preventive measures. A common approach is hydraulic modelling were a design storm is used to simulate an extreme rain event, and the hydraulic response of this can be analyzed. With this tool high risk areas are identified and cities can be built more resilient. To have sufficiently good models and techniques can therefore be crucial for the urban planning in a changing climate. As in all modelling simplifications must be made to enable a cost-effective and timely cloudburst modelling. Common practice today is to simulate cloudburst with spatially uniform design storms of a specific temporal variation called Chicago Design Storm (CDS). Using spatially varied design storms is a feasible and potentially large improvement on current modelling practices. Therefore the question of how much the spatial variation of the rain intensity affects the hydraulic response should be further investigated.

Sweden has seen several cloudburst events in the latest years, with one of the most severe ones occurring in Gävle in August 2021. An intense low pressure caused a heavy cloudburst over the whole Gävleborg area the night between 17th and 18th of August which led to severe flooding in Gävle and neighboring towns. The rain started early on the 17th and intensified in the evening and night, with 161.6 mm registered for the last 24 hours by the Gävle measurement station at 07:00 on the 18th (SMHI 2021a). The event caused large damages to infrastructure and private properties, with reported damages to the insurance companies reaching a cost of almost 500 million SEK over the whole area affected by the cloudburst (Bengtsson 2021). This is one of the most recent, at the time of writing, and intense cloudburst events in Sweden causing severe flooding, making it interesting to use as a case study investigating how the spatial variation of the rain affected the hydraulic response in the city.

1.1 Aims and purpose

The purpose of this project is to investigate how much the spatial variations of intense rains influence the hydraulic response in a city and how well commonly used uniform design storms represent a real rain event. To have a possibility of knowing how modelled results correspond to the actual response a case study is necessary. Since the cloudburst in Gävle, at the time of writing, is the most recent extreme rain event causing severe flooding in Sweden this event is chosen for a case study. Comparison with actual response in the city aims to give a validation of how well the modelled version of the cloudburst represents the reality and radar data from the event is used as a spatially varied rain to investigate.

This purpose is to be fulfilled by answering the following research questions:

- How is the simulated hydraulic response in a model of Gävle with the rain event estimated from radar data in comparison with the real measured response of the actual cloudburst event on the 17-18th of August 2021?
- How is the hydraulic response in the city affected by using a spatially uniform rain with the same temporal variation as the event in comparison with using a spatially varied rainfall input based on radar data from the cloudburst, with the same total rain volume?
- How is the hydraulic response in the city affected by using a spatially uniform rain with a CDS temporal variation, with the same total rain volume, compared with using spatially varied rainfall input from the cloudburst?

The overall aim of the project is to increase knowledge about how to represent precipitation in cloudburst modeling and to contribute to a better and more precise modelling of the hydraulic response in the future.

A limitation of this study is that it only investigates one case with a cloudburst event in Gävle specifically, and does not test if the results are applicable to other places or events. This limits the possibilities to draw general conclusions of the results.

2 THEORY

2.1 Precipitation: formation and types

Precipitation is formed when a moist rising mass of air is cooled down adiabatically and cannot hold the same amount of water vapor. This will lead to condensation of the vapor into cloud drops and a cloud is formed. To fall as precipitation the cloud drops need to grow heavy enough to overcome the force from the upward moving air, which is the condition for the cloud formation. In warm clouds, with temperatures above 0°, this can be done through collision and coalescing of the drops. But in the mid- and high-latitudes, with temperatures usually below 0° in the clouds, there are supercooled water and ice crystals in the cloud working as condensation nucleus. Since the water vapor saturation pressure is slightly lower over the ice crystal this will cause the vapor to sublimate on them and they will grow in size and eventually become heavy enough to fall down and reach the ground either as snow, or if the air under the cloud is above freezing temperature

as rain (Hendriks 2010; Stull 2017).

There are different types of precipitation, characterized by the air rising process. The type that typically is the most intense is convective precipitation (Hendriks 2010). A convective rain formation process is showed in Figure 1 and is a result of air close to the ground being heated faster than the air higher up in the atmosphere, which leads to temperature in the vertical direction changing quicker than the adiabatic lapse rate.

The lapse rate, Γ, is how fast the temperature decreases with altitude, $\Gamma = \frac{-\Delta T}{\Delta z}$, and if this decreases without any heat exchange with the environment it is called adiabatic lapse rate. For dry air the adiabatic lapse rate is Γ_d = 9.8 C°/km. When the environment lapse rate changes quicker than the adiabatic lapse rate the atmosphere is in an unstable condition since an air parcel rising from the ground, cooling adiabatically, will cool down slower than the atmosphere and thus be warmer than it's environment and get pushed upwards (Stull 2017). Movements in the atmosphere are amplified during this condition which can cause large amounts of air to rise and form clouds and possibly cloudbursts. These conditions commonly occur during sunny summer days when the ground is heated rather efficiently compared to the atmosphere above (Dahlström 2010). This type of rain accounts for most of the short-term extremes with durations under one hour in Sweden and they are formed in situations when the atmospheric instability is high and deep convection occurs (Dahlström 2010). Niemczynowicz (1984) summarised from different studies that the convective rainfall cell on average is 1-5 km^2 in size.

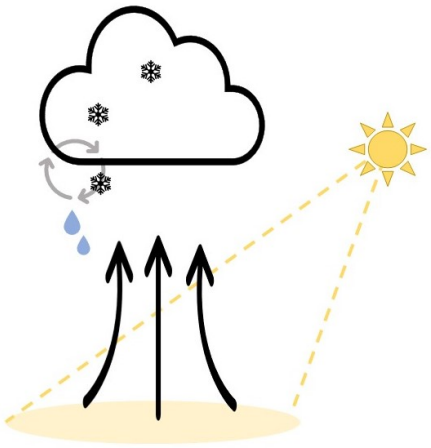

Figure 1: The convective rain formation process.

Other types of precipitation are orographic, frontal and cyclonic. Orographic precipitation is formed when an air mass is forced to rise due to the topography (Hendriks 2010). Frontal precipitation is formed when large cold or warm air masses meet and the warm air is forced to rise above the cold air; the frontal rain is generally characterised by a low intensity but instead a long duration since the air can rise rather slowly over a front which in itself also can be very slow-moving (Dahlström 2010; Hendriks 2010). Cyclonic precipitation is caused by the uplift of the air in the center of a low-pressure area where the air is converging, since air is flowing form high pressure to low pressure areas (Hendriks 2010). This leads to a lot of air meeting in the centre of the low pressure area, being forced to rise, and the cloud and precipitation formation process described earlier can start to take place. The different precipitation types can also be combined and amplify each other (Hendriks 2010). The convective cells can for example occur isolated, but they are quite commonly embedded in a front and then combined with frontal rain (Dahlström 2010). The frontal and the cyclonic precipitation occurring together in large-scale weather systems are also common in the mid-latitudes, which most of Sweden belongs to (Hendriks 2010).

2.2 Extreme weather and heavy rainfall in a changing climate

Extreme weather events are by definition rare and include weather events that are unusually intense or long for that place or season; they can also be defined by their effect on the society or the physical environment. Examples of this are unusually many days of drought, unusually high or low temperatures or unusually long lasting or intense rains (SMHI 2021b). What can be called an extreme weather event is different for every place depending on climatic conditions and on sensitivity to specific weather events. Intense rains are often causing problems with flooding, especially in urban areas. SMHI (2021c) defines a rain event as extreme if the intensity exceeds 50 mm/h or 1 mm/min, but also points out that rains of over 40 mm/24 h will be perceived as extreme and can be called cloudbursts.

Climate statistics is used to define a weather event as extreme based on it being rare for that place and season, and events are compared with the weather averages and variations of that place. The concept return period, referring to the average time between events, is often used to define how likely a specific weather event is, which also implies how extreme it is. For example, during one year, a rain intensity with the return period of 10 years has the probability of 1/10 to be exceeded and a rain with the return period 100 year has the probability of 1/100 to be exceeded (SMHI 2019) and these rain intensities are often referred to as a 10-year rain event or a 100-year rain event. The accumulated risk over a period is however different, the risk of a 100-year event to occur or be exceed during 100 years is 63%.

The climate statistics and climatic averages that the current definitions of extreme weather have been based on are however changing with the human driven climate change, and what was an extreme and quite rare event might become more common in the future. IPCC (2021) states that there is a general increase in heavy precipitation in the world since the 1950s that is likely to be driven by human-induced climate change. Specifically in Northen Europe the results show with a high confidence level that the precipitation in the area has increased due to human activities. The heavy precipitation is also according to the IPCC (2021) very likely to become more frequent and intensify with an increasing global temperature; for example the intensity of extreme daily precipitation events is with high confidence estimated to increase by 7% for every degree of global warming, following the Clausius-Clapeyron relationship.

However Olsson et al. (2017) that studied extreme precipitation events specifically in Sweden could not yet find any obvious trend in the magnitude or frequency of the cloudbursts over the period 1996-2017, but there is a possibility that the lack of trend is due to the rather short time period with available data from automatic measuring stations. A little increase could be seen though on the annual highest observed rainfall depth since 1881. It is estimated in the report that the future extremes will be 10-40% more intense, depending on the emission scenario and time horizon. This implies that a climate factor of 1.1-1.4 should be used for dimensioning volumes, which is in line with the suggestion from Svenskt Vatten (2020) of a climate factor of 1.25 for rains with shorter durations and 1.2 for longer rains when studying events in the end of this century. A climate factor is a factor used to multiply the rain volumes with when studying events in the future to account for the estimated precipitation increase.

2.3 Flooding

Flooding events can be classified in different ways, and three common types are coastal, fluvial or pluvial flooding. Coastal flooding occurs when the sea level is rising or storms are pushing sea water ashore. Fluvial flooding occurs when the lake or river water levels are rising so much that the surrounding land is overflowed, which can be due to large amounts of rainfall, often from long lasting rains, or snowmelt. Pluvial flooding on the other hand is happening more instantaneously when a rainfall rate is higher than the grounds infiltration capacity and water starts to flow on the ground, so called Hortonian overland flow, named after Robert E. Horton. This can happen also in a short rainfall if the intensity is high enough. In dry areas of the world, Hortonian overland flow can be a significant part of the runoff process when heavy rainfall occurs since the ground usually is harder after dry periods. In Sweden however, with a lot of till and a rather wet climate, the infiltration capacity of the ground is most commonly higher than the normal rainfall intensity (Grip & Rodhe 2016). Pluvial flooding happens in extreme rainfall events though, and especially in urban areas where the infiltration capacity of the ground is significantly impaired by a lot of hardened surfaces. Here the stormwater drainage systems are instead determining how intense rain the area can handle without being flooded. The Swedish stormwater systems are recommended to be dimensioned for a 10-year rain event in central parts of a city, which means that a rainfall with higher intensity than the system can handle will statistically happen every 10 years (MSB 2013).

Kaspersen et al. (2017) found in their study that both climate change and urban development increases the risk of pluvial flooding in European cities, and the relative importance of these two varied between different cities.

2.3.1 Pluvial flooding events in Sweden

Globally flooding events are causing a lot of damage every year and are estimated to kill on average 5400 persons every year (MSB 2012). In Sweden flooding events rarely leads to deaths, even though it has happened, but the floodings do regularly cause damage on buildings, infrastructure and valuable nature and cultural heritage. MSB (2012) did an inventory of severe flooding events in Sweden 1901-2010 and found 190 flooding events of importance. A great majority of the flooding events in Sweden are fluvial and pluvial, with fluvial events due to long-lasting rainfall or snowmelt being the most common (MSB 2012). Pluvial flooding, the second most common type, is an effect of extreme rainfall and is often hard to predict due to the convective and short-term nature of these rains.

Examples of pluvial flooding events in Sweden causing great damage are:

- The cloudburst in Malmö 2014-08-31 with 122 mm falling during 6 hours, where the intense rain were centered over the central parts of the city (Hernebring et al. 2015). The cloudburst and flooding caused severe damage and the cost of this was estimated to over 300 million sek.

- The cloudburst in Uppsala 2018-07-29, connected to a thunderstorm, with 82 mm falling in a short amount of time (Forsell 2018). This rain was also causing great damage and costs for the municipality, with for example the passage under the train station being filled with water and parts of the hospital needing to shut down for some days due to flooding (Carpman 2018).

- The cloudburst in Gävle 2021-08-17 to 2021-08-18, where the automatic measuring station registered 161.6 mm during 24 hours (SMHI 2021a), breaking both records and infrastructure. This event holds the record for the highest measured rainfall depth in Sweden for durations of 2-12 hours since the measurements on shorter periods than a day started in 1995, with for example 101.9 mm falling during 2 hours and 136.3 mm falling during 6 hours (SMHI 2021d).

2.4 Design storms and cloudburst modeling

Heavy rainfall events are becoming increasingly common and intense and urbanization is increasing flooding risk by hardening surfaces and with expansion of cities out on less suitable areas due to lack of space. A measure used to predict areas that risk being flooded in a cloudburst event is to do simulations of heavy rainfall in a cloudburst model and map risk areas. This can be done on different levels: only mapping low-points, mapping including surface runoff and mapping including both surface runoff and stormwater system (MSB 2017).

Mapping of low points

This is the simplest type of cloudburst mapping only including an elevation model of the ground and buildings over the area being mapped. A software handling Geographical Information Systems (GIS) is then used to identify low points and flow paths between these points. The mapping is rather easy to perform and gives a good overview of where problems can occur, but it is not a real cloudburst mapping since the results are not connected to a specific rain intensity or volume (MSB 2017).

Mapping of surface runoff

This method uses, except for the elevation model, a 2D hydraulic model describing how the water flows through the catchment and accumulation in low points downstream. In this method rain is simulated in the model and infiltration and friction of different surfaces are included, which gives a more realistic view of the flooding scenario and a possibility to study rains of different return periods, durations and intensity variations. But the stormwater system capacity is in this method simplified as a deduction of the rain input. This makes the method rather unsure to use for rainfall volumes close to the stormwater system capacity, since this is difficult to estimate exactly, and it is recommended to use at least a 100-year rain for the simulations. This is a rather cost efficient method to get a view of which areas will be flooded by different rain volumes (MSB 2017).

Mapping of surface runoff and stormwater system

The most exact but also the most resource demanding method is to map the surface runoff and include the stormwater system. The 2D hydraulic model is then connected to a 1D hydraulic model for the stormwater system. This can also be done on different precision levels from just including the water mains to including every pipe in the system. With this method both more general and detailed studies can be performed, but the model needs to be more detailed the lower the studied rain volumes are, since the stormwater system has a larger impact on the runoff in those cases compared to in an extreme rain event (MSB 2017).

2.4.1 Recommendations for cloudburst mapping

The elevation data need to have a sufficiently high resolution to get acceptable results from the cloudburst mapping. MSB (2017) recommends a resolution of at most 5×5 m cells for an urban area, to be able to describe important urban structure accurately. The elevation data needs to be modified with elevation of the buildings and lowering at bridges, viaducts and other places where water in the reality flows under the surface described by the uncorrected elevation model. Culverts along dikes have a rather small capacity, and can in more general studies be left uncorrected.

The infiltration capacity and flow resistance of the ground is recommended to be included in the model with different values for hardened and non-hardened surfaces, extracted from land use data. A soil type map can be used to more accurately find the infiltration rate for the different surface materials in the area (MSB 2017).

The stormwater system can in a surface runoff model be accounted for by subtracting it's capacity from the rain volume input. The recommended stormwater system capacity is for a 10-year rain in central parts of a city, 5 year rain in densely built-up areas and for a 2 year rain in more sparesly built-up areas (Svenskt Vatten 2016).

2.4.2 Design storms

Design storms are used to perform cloudburst mapping where rain events are simulated. Rainfall statistics is needed to construct a design storm, preferably from the specific place that the design storm will be used for. The rainfall statistics has traditionally been available in the form of block rains, which means that only information about the mean intensity of the rain for a specific duration and how often it occurs is available. From these statistics intensity-duration-frequency relationships are derived, and can be used to find the statistical frequency of a rain with a specific intensity and duration, or the intensity of a rain with a specific duration and return period (Svenskt Vatten 2011). Based on Swedish precipitation statistics Dahlström (2010) have further developed an already existing formula for the relation between rain intensity, duration and frequency, a so called IDF-function, that is now valid for rain durations up to 24 hours. This formula is presented in Equation 1 with I = rain intensity [l·s^{-1}ha^{-1}], R = return period [months] and D = rain duration [minutes], and is the IDF-function recommended for Swedish conditions for rain durations up to 24 hours (Svenskt Vatten 2011).

$$I = 190 \cdot \sqrt[3]{R} \cdot \frac{ln(D)}{D^{0.98}} + 2 \tag{1}$$

With this formula the frequency, i.e. the return period, for different rain events can be determined. The IDF-function tells nothing about the temporal or spatial variations of the rain, just the relation between mean intensity for a duration and the frequency of this.

2.4.3 The Chicago Design Storm

Design storms are normally simplified as uniform spatially, but not temporally. A classic temporal variation to use for design storms is the so called Chicago Design Storm (CDS), which is originating from a method of generating design storms presented by Keifer &

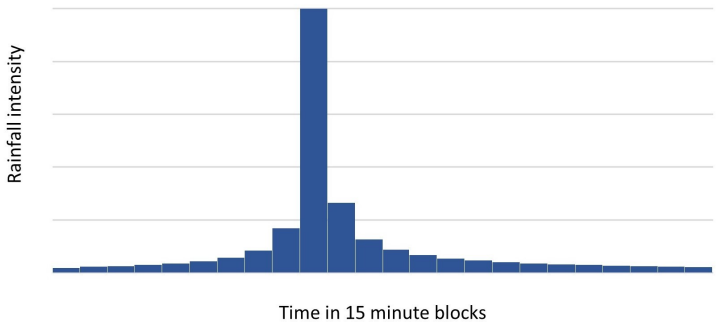

Figure 2: A CDS hyetograph with 15 minute blocks, a unitless rainfall intensity and a duration of 6 hours.

Chu (1957) in Chicago, and that has been widely used and adapted for different conditions all over the world. A hyetograph is a graph describing the rain intensity varying with time. The important characteristic of the CDS hyetograph is that it, for a specific return period, includes the intensities for all different durations up to the total duration of the CDS-rain. It consists of a set of block rains where the most intense 15 minutes represent the mean 15 minute intensity for that return period, and the most intense hour have the mean 1 hour intensity for the return period (Svenskt Vatten 2011). This is convenient since several durations can be simulated with just one design storm, but it also gives the hyetograph a rather unrealistic pointiness with a large part of the rain volume falling during a short amount of time, which can cause the runoff peak to be overestimated. An example of a unitless CDS hyetograph is presented in Figure 2 where the characteristic pointiness can be seen. When the peak intensity occurs during the rain event has an effect on the result and Arnell (1982) finds that r, which is representing time to the peak divided by total duration, for a CDS evaluated with data from Göteborg range from 0.3 to 0.48. For return periods shorter than 1 year r was on average 0.43 and for return periods of 1-10 years r was on average 0.35 (Arnell 1982).

2.5 Spatial variation of intense rains and it's effect on modelled results

A model is never better than it's input. Rainfall, the most important input in cloudburst models, is commonly applied as a spatially uniform rain in modelling of runoff for smaller areas. This has in several studies been proven to be insufficient for a correct estimation of the runoff, since real rainfall is not spatially homogeneous in intensity. Segond et al. (2007) explored the effect from spatial variations of the rainfall through comparing the modelled runoff response from a uniform catchment rainfall based on a single rain gauge with spatially varied rainfall from radar data and from a set of rain gauges. They found a clear decrease in model performance when using the uniform rainfall compared to the spatially varied one, especially with an increase in spatial variability of the rain intensity which for example happened in more intense summer events. Faurès et al. (1995) conclude that the spatial variability of the rainfall can create large variations in the modelled runoff even in a small catchment of only 0.044 km^2 and Goodrich et al. (1995) find in the same catchment, which is situated in an area with convective rain, that rainfall depth varies by 4-14% between measuring points only 100 m apart. Specifically convective rains have a larger spatial variability, which is pointed out by Bell & Moore (2000). They concluded that convective rains have twice the spatial variability compared to stratiform frontal rains, even when they create a similar peak flow, which also makes the simulated

runoff results more sensitive to the spatial variations during convective rain. Convective rains are mentioned specifically in this section since they are often intense, but in the case of the Gävle cloudburst there was probably an intense low pressure causing the rain and not a convective process.

The spatial variability has also been found to have a connection to the return period and the intensity of the rain. Peleg et al. (2017) used a model in a small urban catchment in Switzerland to simulate rainfall for a 30 year period from a stochastic spatially distributed rainfall generator, which would include both the spatial variability of the rainfall and the climate variability. They concluded that the spatial rainfall variability and it's effect on the runoff became more pronounced with longer return period. This means that taking into account the spatial variability of the rain might be more important when doing flood risk assessments, for which rains with longer return periods will be simulated, compared to for example simulations for stormwater system dimensioning. Also Fiener & Auerswald (2009) found that the spatial variation of the rain increased with the intensity, and that the intensity in the studied case (4 years of measurement from 13 gauges within 1.4 km^2 in southern Germany) varied by 1- 15.7 mm/km with a mean of 4.2 mm/km. They conclude that the assumption of a spatially uniform rainfall is invalid even at a sub-kilometer scale, especially in investigations focusing on intense and rare rain events. Maier et al. (2020) have similar conclusions after studying the spatial rainfall variability in a larger urban catchment. They found that the spatial variability of the rainfall was higher with higher intensity of the rain, and their results showed that for rains with $>$17 mm/h in intensity, often convective summer storms, the coefficient of correlation was very low between the different rain gauges, only 0.19. While for rains $<$17 mm/h the coefficient of correlation was of at least 0.83 between the gauges.

Urban areas are more sensitive to rainfall in their runoff response due to an increased amount of hardened surfaces and improved flow paths on roads (Skougaard Kaspersen et al. 2017), pipes etc, especially since the urban catchments often are small. This also makes them more sensitive to spatial rainfall (Segond et al. 2007). Segond et al. (2007) found that the catchment response time on average decreased by 50% when subcatchments where artificially urbanized.

Even though several studies show that the spatial variability of the rainfall has significant impact on the modelled hydraulic response and there is a large number of researchers questioning the assumption of a uniform rainfall in modelling, there are also studies concluding that the temporal resolution, and then also variability, affects the results more strongly than the spatial resolution (Krajewski et al. 1991; Ochoa-Rodriguez et al. 2015). Brath et al. (2004) concluded that with a reliable estimation of the areal rainfall, based on a sufficiently dense rain gauge network, models can perform well also with a spatially uniform rainfall input. To use a uniform rainfall input is simpler and less computationally demanding, which means that if models can perform sufficiently good with this input it is the better alternative. It is therefore relevant to further investigate the question of the effect of the spatial variability of rainfall intensity on modelled response.

2.6 Hydrodynamic modeling in MIKE 21 Flow Model FM

MIKE 21 Flow Model FM is a 2D-model developed by DHI, mainly for marine and coastal application, but it is also suitable for simulations of flows over land and flooding (DHI 2020a). FM stands for Flexible Mesh, and by using a flexible mesh the model can include larger areas since the resolution of the mesh can be adapted depending on the properties and importance of different parts of the model area. The model works by finding the numerical solutions to the 2D Navier-Stokes equations describing the exchange between all the elements in the flexible mesh (DHI 2017). The modelling in MIKE 21 Flow Model FM consists of different modules, where the *Hydrodynamic only* module is obligatory and the module *Inland Flooding* can be chosen to simulate flows over land (DHI 2017).

2.6.1 Domain and time

Except for choosing which module to use basic parameters as *domain* and *time* needs to be chosen. The domain is set by connecting a mesh to the model covering the model area and with information about the elevation. The mesh is generated in MIKE Zero Mesh Generator, where the resolution for different areas and the boundaries are chosen. The software MIKE Zero is the graphical interface used to set up the simulations and pre-process the data (DHI 2020b). MIKE 21 is included in the MIKE Zero framework and can be used from this interface, and the results from MIKE 21 can be opened and analysed in MIKE Zero. The mesh is the most important input to the model; it needs to describe the surface elevation well enough but also give reasonably long computational times. To achieve this a triangular mesh is created with triangles without too sharp angles and with a high resolution only in areas where the results are of interest. The mesh is called flexible since different resolutions can be chosen for different parts of the model depending on the aims of the study. In mesh generator different identities are given to the boundaries, which later in the *Boundary conditions*-section of the hydrodynamic module is translated to boundary conditions (DHI 2017). Boundaries can be closed or open, which include options as free flow, specified discharge or specified level (DHI 2017).

In the *time*-section the simulation period is chosen as well as the general time step. This determines how often output is generated, but the model can use smaller time steps than this to keep the stability condition (DHI 2017). The range of the time steps the model can take are chosen within the hydrodynamic module in the section *solution technique* where a minimum and maximum time step is chosen. The minimum time step needs to be small enough for the model to keep the stability condition, but a small time step will also increase the computational time. The model uses the Courant-Friedrich-Lévy (CFL) number to determine how small time step it needs to take to keep the stability and a CFL-condition is set in the Solution Technique-section and should be set below 1 (DHI 2017). The CFL-number increases by smaller elements in the mesh and decreases by smaller time steps. Hence, the model will have to use smaller time steps when the model elements are smaller to keep the CFL-condition.

2.6.2 Infiltration and bed resistance

How the flow is affected by the friction from different surfaces, and the infiltration into the ground on different surfaces can be included in the model in the sections *bed re-*

sistance and *infiltration*. The bed resistance can be defined by either Manning number, Chezy number or by a wave induced bed friction and as temporally and spatially constant or varying (DHI 2017). A high Manning number M is associated with a low roughness of the ground and higher flow velocities. In English literature the inverse of Manning number, Manning's roughness coefficient $n=\frac{1}{M}$ is often used instead. Values of Mannings number for different surfaces recommended by Vägverket (2008) and MSB (2014) are presented in Table 1.

Table 1: Manning numbers from different surfaces (MSB 2014; Vägverket 2008)

Manning number, M [m$^{1/3}$/s] , recommended by Vägverket (2008)	
Smooth asphalt	80-85
Rough asphalt	70-75
Gravel	40-50
Short grass	30-35
Long grass	25-30
Manning number, M [m$^{1/3}$/s] , recommended by MSB (2014)	
Green area	2
Impermeable surface	50

The infiltration can be included in two different ways in MIKE 21, either as a *Net infiltration rate* or as a *Constant infiltration with capacity*. While the infiltration rate in the first approach is set to either constant or time varying, it is in the second approach constant in time but can be defined as varying over the domain. With the second approach an infiltration zone is defined by depth, porosity and with an initial water content and then infiltration rate, the flow from the surface down in the unsaturated zone, and leakage rate, the flow from the unsaturated zone to the saturated zone is set (DHI 2017). With this the model can take into account a previous rainfall leading to decreased storage capacity. MSB (2014) suggests 36 mm/h as a reasonable value of the infiltration rate for a thin layer of topsoil on moraine basis. The infiltration rate is of a similar magnitude in moraine, topsoil and filling material, common in urban areas (MSB 2017).

2.6.3 Sources, precipitation and other model selections

To include inflows to the study area *sources* and *precipitation- evaporation* must be defined. The section *sources* is suitable for including a watercourse crossing the model borders and adding water to the model area, and the discharge can be defined either as constant or varying in time. To simulate rainfall a file with the rain intensities must be added to the project in MIKE Zero. The rain intensity can be added as either a time series or a constant and applied homogeneously over the whole area or with specific series associated with different grid cells (DHI 2017). Evaporation can also be included in this section as a negative precipitation.

Flooding and drying depth needs to be specified to define when areas are flooded, dry or partly flooded in the model, which determines if a model element is included in the calculations or not. An element with a water depth above the flooding depth is counted as flooded and both mass and momentum fluxes are calculated for this. An element with water depth below the flooding depth is counted as dry and no calculations are done. If the water depth of an element is between the flooding and drying depths the element is counted as partially flooded and momentum fluxes are set to zero but mass fluxes are

calculated; it can also be counted as partially flooded if the water depth is below the drying depth but a neighboring element is flooded. Very low values of the flooding depth can cause stability problems and for inland flooding the drying depth is recommended to be in the range of 0.001-0.02 m and the flooding depth is recommended in the range 0.002-0.05 m (DHI 2020a).

3 MATERIALS AND METHODS

The research questions are to be answered by making a 2D hydraulic model using MIKE 21 Flow Model FM and analyse the results of different type of precipitation input in the model. Precipitation input are based on radar data provided by SMHI corrected against the Gävle measurement station. The stormwater system is accounted for by making a deduction of the precipitation input corresponding to it's capacity, on surfaces assumed to be connected to the stormwater system. This is the method recommended by MSB (2014) when cloudburst are analysed since these have large intensities compared to the stormwater system capacity, which means the uncertainties in the deduction will be small in relation to the precipitation input. All the spatial data are in the SWEREF99 TM coordinate system with the vertical reference system RH 2000, and all the time indications are given in UTC.

3.1 Study site and model area

The city Gävle in Sweden was chosen for this study due to the extreme rainfall event taking place there in August 2021. Gävle has 103 000 inhabitants in the municipality and 75 000 in the city (SCB 2021), situated on the east coast of Sweden. The river Gavleån flows through the city, west to east, out in the Gävle bay and the river Testeboån flows north to south, passing parts of the city before entering the Gävle bay. The borders of the model area were chosen so the catchments of the small watercourses, without information about the discharge available, entering the city from the south and the north were included. With the catchments for the small watercourses included in the model area these were not necessary to include as sources in the model. However the large catchments of Gavleån and Testeboån were cropped since these otherwise would make the model far too large for this study, and also the catchments of the smaller watercourses Bäckebrobäcken and Kungsbäcken since values of the discharge in these watercourses were available and could be included as sources. Bäckebrobäcken flows through the north west part of Gävle, called Sätra, before entering Gavleån and Kungsbäcken enters Gavleån from the south, rather close to the model border. These watercourses are marked in Figure 3 with red dots where they are crossing the model border.

This chosen model area had a total area of 54 km^2, which is a large model for simulations in MIKE. To reduce computational time of the simulations the model area was parted in two through Gavleån, northern and southern Gävle which then got the areas 18 and 36 km^2 respectively and should not have any exchange of water. To further reduce the computational time a flexible mesh was used so low resolution could be applied to areas of less importance for the results but that still contribute to the overall flow in the model.

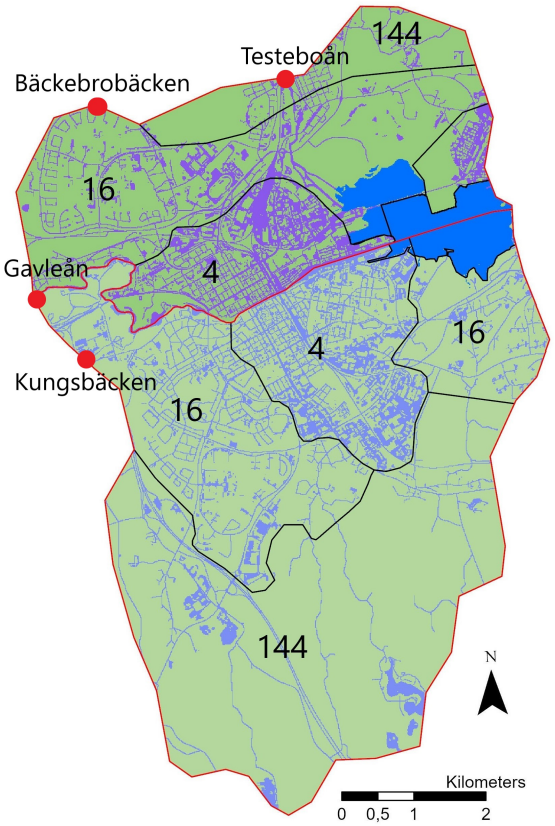

Figure 3: The northern and southern model area with borders in red, and parting between different resolution areas in black with resolution given in m^2. Background map is based on land use data from GSD-Property map ©Lantmäteriet.

The central parts of the city, more sensitive to pluvial flooding with a lot of hardened surfaces were assigned a resolution of 4 m^2, the urban but less central parts were given a resolution of 16 m^2 and the rural parts were given a resolution of 144 m^2. Only the central parts of the model, in the city, is of interest for evaluation and the more rural parts are included with a lower resolution only since they are contributing to the flow in the central parts. The urban area, relevant for evaluation, have a higher resolution than 25 m^2 per cell, which is in line with recommendations from MSB (2017) presented in section 2.4.1 and also in line recommendations by Xing et al. (2019) that studied the effect of digital elevation model (DEM) resolution in urban flood modelling. The model areas and their parts with different resolutions are shown in Figure 3.

3.2 Model setup

3.2.1 Domain and mesh

The basis in the model is a topography, or in MIKE called bathymetry, containing the elevation of every grid cell in the studied area. This was prepared in ArcGIS and SCALGO Live and a DEM of the area with data from Lantmäteriet, GSD- elevation data with 1×1 m resolution and property map, was used. The DEM was corrected with removing of bridges, viaducts and surface over culverts in SCALGO Live to more correctly describe flow paths, and the buildings were elevated by 2 m in ArcGIS, according to recommendations presented in section 2.4.1. This was loaded in MIKE Zero Mesh Generator with a 2×2 m resolution and in Mesh Generator the model boundaries were drawn as well as partitioning into areas with different resolutions; the resolutions are chosen in the areas

as the maximum allowed element size in the mesh. The mesh created from the corrected DEM was loaded into the domain-section in the MIKE model and the boundary around the the model areas where chosen as closed, except for at the sea where an open boundary with a free outflow was set. Since the model boundary was chosen so it is on the city side of the watershed border, which means all the water in the model flow towards the sea or first towards Gavleån and then towards the sea, a closed model boundary should not cause water to be gathered at the border. After uncertainties about if the free outflow-condition set at border towards the sea was working properly a lowering of the elevation at the sea was made by -2.5 m, starting around 10 m out from the coast. This is making the sea in the model act as a large sink where water can be gathered, without affecting the flooding on land, which is what is being studied in this case. This was done to ensure unaffected results even if the free outflow-condition is not working.

3.2.2 Simulation time and solution technique

The simulation time was chosen based on when the most intense raining occurred and on the time of concentration in the model area. The rainfall rate started to pick up around 20:00 and the peak of the rain intensity occurred 21:30 to 00:30, with the maximum intensity occurring between 23:00 and 00:00. The time of concentration, i.e. the time it takes for rain falling in the most distant parts of the catchment to reach the point of interest, was used to estimate for how long time after the peak of the rain intensity the depressions keep being filled and simulation should be running. The longest time of concentration was estimated, by studying flow paths in SCALGO Live, to be around 6 hours for the southern model area and 3 hours in the northern model area. The simulation time was chosen so at least 6 hours after the peak was included to make sure the flooding peak was included in every part of the modelled area, but was also extended to include moments that validation data was available from. The simulation time was based on this chosen to be 20:00 to 9:45. To account for the effect of the low intensity rain falling before 20:00 during the full day of the 17th of August a pre-rain, 00:00-20:00, based on radar data from the event is simulated giving the saturation in the ground to use as initial water content input for the rest of the simulations.

3.2.3 Other choices and input parameters

The parameters flooding and drying depths, determining which elements to be included in calculation of fluxes, were set to 8 and 10 mm, which is within the range recommended by DHI (2020a) presented in section 2.6. The time step range was set to 0.001 to 30 seconds and a CFL-condition of maximum 0.8 to avoid stability problems. Both bed resistance and infiltration were chosen as constant in time but varying in domain. The study area were parted into hardened and non-hardened surfaces in ArcGIS based on land use data from Lantmäteriet, and grids assigned with different values for Manning number and infiltration parameters were created, which is the recommended method by MSB (2017). The model area parted into hardened and non-hardened surfaces can be seen in Figure 3 with hardened surfaces in purple and non-hardened in green. Manning number were chosen as 2 for non-hardened surfaces and 50 for hardened surfaces, which is what MSB (2014) recommends for these type of surfaces. These are lower values on M than the ones recommended by Vägverket (2008) which were presented in Table 1. A summary of the input parameters can be seen in Table 2.

Table 2: Input parameters for the hydraulic modeling

Parameter	
General time step	30 s
Time step range	0.001- 30 s
Manning number non-hardened	2 $m^{1/3}/s$
Manning number hardened	50 $m^{1/3}/s$
Flooding depth	0.01 m
Drying depth depth	0.008 m

The infiltration type was set to constant infiltration with capacity, which demands information of the depth and porosity of the infiltration zone and the initial water content in the zone given as percentage of the capacity. This together with infiltration rate and leakage rate of the infiltration zone, that are all needed input parameters for the infiltration module are presented in Table 3. These parameters were also included in the model from a grid file, separating between hardened and non-hardened surfaces and with different layers for the five parameters. The infiltration rate was set to 36 mm/h which is suggested by MSB (2014) for a thin layer of topsoil on till basis and MSB (2017) states that infiltration rate is of a similar magnitude in till, topsoil and filling material which are common in urban areas. Studying a soil type map shows that till is the most common soil type around Gävle.

Table 3: Input parameters for the infiltration module

Parameter	**Non-hardened surfaces**	**Hardened surfaces**
Infiltration rate	36 mm/h	0.001 mm/h
Leakage rate	0.40 mm/h	0.01 mm/h
Porosity	0.40	0.01
Depth of layer	0.30 m	0.01 m
Initial water content 00:00	20 % of capacity	20 % of capacity
Initial water content Northen 20:00	44% of capacity	44 % of capacity
Initial water content Sothern 20:00	49% of capacity	49% of capacity
Initial water level Northen	-2.5 m	-2.5 m
Initial water level Southern	-2.5 m	-2.5 m

The initial water content at 00:00 2021-08-17 for the model simulating the pre-rain was set to 20% based on the fact that the cloudburst took place in August when the ground is generally rather dry and to make it comparable with other degree projects within the same subject using this value (Elfström & Stefansson 2021; Olsson 2019). For the rest of the simulations, starting at 20:00, the simulated saturation in the ground after the pre-rain was used as the initial water content. In the northen model the saturation in the ground reached on average 44% at 20:00 and in the southern model it reached on average 49%. The initial water level is set so it is just below the lowest point in the elevation model, which otherwise would start with standing water. Values for the leakage rate, porosity and depth of layer were all based previous studies using these (Elfström & Stefansson 2021; Olsson 2019).

3.2.4 Sources

The rivers and the small streams whose catchment areas are not fully within the model area are included as point sources where they are crossing the border to the model area. These are Gavleån, Testeboån, Bäckebrobäcken and Kungsbäcken, and modelled daily

values of the discharge in these from 2021-08-17 and 2021-08-18 are available from SMHI's hydrological model S-HYPE. The discharge did not differ much between the days so it was, for all the watercourses, included as a constant source with the average value of the discharge from the two days on the point where the watercourse crossed the model boundary. The discharge available from S-HYPE are modelled for the outlet of the watercourse, and was adjusted by multiplying with the ratio of the catchment area being situated outside the model area and the total catchment area; the information about these areas were taken from SCALGO Live. The elevation model does include the surface of the watercourses, and since there is no information about the discharge when the elevation model was created this is assumed to be the surface with a mean discharge in the watercourses. To correct for this discharge already being included, the mean discharge in the watercourse was subtracted. The corrected discharge, Q, was calculated according to Equation 2 and the results that were used as constant point sources in the model are presented in Table 4. The positions of the point sources are marked in Figure 3.

$$Q = \left(\frac{Q_{17/8} + Q_{18/8}}{2} - Q_{mean} \right) \cdot \frac{\textit{Area of contributing part}}{\textit{Area of whole catchment}} \tag{2}$$

Table 4: Discharge in the watercourses included as sources, corrected according to Equation 2 (SMHI 2021e)

Watercourse	**Corrected discharge Q [m^3/s]**
Gavleån	15.85
Testeboån	2.04
Bäckebrobäcken	3.05
Kungsbäcken	7.41

3.3 Precipitation input

Radar data with the estimated precipitation over the Gävle area from 2021-08-17 00:00 to 2021-08-19 00:00 was provided by SMHI with a 15 minute and 2×2 km resolution. The reflectivity was already converted to a rainfall rate given in the unit mm/h, but not corrected against the automatic measurement station in the area.

Radars have the advantage compared to rain gauges that they can capture the spatial variability of the rainfall and cover large areas; however they are often insufficient in accuracy since radar measurement is indirect with rain intensity being derived from the measured reflectivity (Ochoa-Rodriguez et al. 2019). The accuracy of radar rainfall estimates can be improved with various gauge-based adjustments, often called radar-rain gauge merging. The rain gauge measurement is then assumed to be the correct rainfall at the gauge's location and the radar data is assumed to have the correct spatial variation and by merging information from these two sources a more correct rainfall field can be estimated. One way to to this is with a mean field bias adjustment of the radar data.

3.3.1 Mean field bias adjustment of radar data

The mean field bias adjustment (MFB) is a simple, but also the most common, adjustment technique in radar meteorology (Q. Qiu et al. 2020). This method assumes that there is a

uniform systematic multiplicative error in the radar data, introduced in the radar rainfall estimates from the reflectivity, and thus that this error can be decreased by multiplying all the radar data with a factor correcting this bias (McKee & Binns 2016; Ochoa-Rodriguez et al. 2019). The correction factor C can be derived from Equation 3 where G is the gauge measured rainfall rate at location i and R is radar rainfall estimate at location i (McKee et al. 2018).

$$C = \frac{\Sigma G_i}{\Sigma R_i} \tag{3}$$

This correction factor C is then applied to the full radar field, $R_{corrected} = C \cdot R$. The comparison, G/R, the correction is based upon is done for a specific time step, for example hourly or daily, over which the radar and gauge data is accumulated or averaged. Smith et al. (2007) conclude that the relation between rainfall rates and reflectivity is temporally varied and thus that a dynamic correction factor is needed to correct the radar rainfall estimates, which implies that time steps should not be set as too long, making the adjustment nearly static. Thorndahl et al. (2014) found that a mean field bias adjustment in general is a correction method giving sufficiently good results, but also that specifically an hourly MFB, based on hourly accumulated values of the rainfall, performs better than a daily MFB and give a better estimation of both rainfall and peak. An example from an extreme rain event, the Copenhagen 2011 cloudburst, is tested with the different bias correction time steps and it is concluded that a daily MFB will underestimate the rainfall, and that an hourly MFB improves the estimation even more when the rain event is intense. There are also other studies confirming that a higher temporal resolution improves the MFB correction, for example hourly compared to daily or event-length time steps (Hanchoowong et al. 2012; Wright et al. 2014) and several studies using an hourly MFB, confirming it as a relevant correction method (Smith & Krajewski 1991; Wardhana et al. 2017). This is motivating the choice of an hourly MFB which have been used as a correction method for the radar data from the Gävle area.

3.3.2 Correction of the radar data from Gävle

In Gävle there is an automatic measuring station, station number 107420 positioned at 60.7161 °N, 17.1607 °E, controlled by SMHI, measuring the accumulated rainfall volume every 15 minutes in the unit mm. Multiplying these values by 4 is giving the average rainfall intensity in mm/h for these 15 minutes instead. This station is positioned approximately where four radar grid cells meet and the rainfall data from these four cells, weighted with the relative distance between the radar cell center and the measurement station, are used in the comparison and correction with the station data.

The measured rainfall from the SMHI station and the estimated rainfall, weighted from the four radar cells over the 48 h 2021-08-17 and 2021-08-18 are presented in Figure 4. In the plot it can be seen that the radar data follows the pattern of station data well, but in the peak it is significantly lower than the measurement from the station.

The correction factor aims to correct a general bias, which is why an hourly MFB is applied and not a shorter time step. The hourly average rainfall intensity from the radar estimation and the station measurements were created and saved as vectors, and then the data pairs where both vectors had values exceeding 0 were seen as valid and used to generate a correction factor as in Equation 3. For the time steps with zero-values in one or

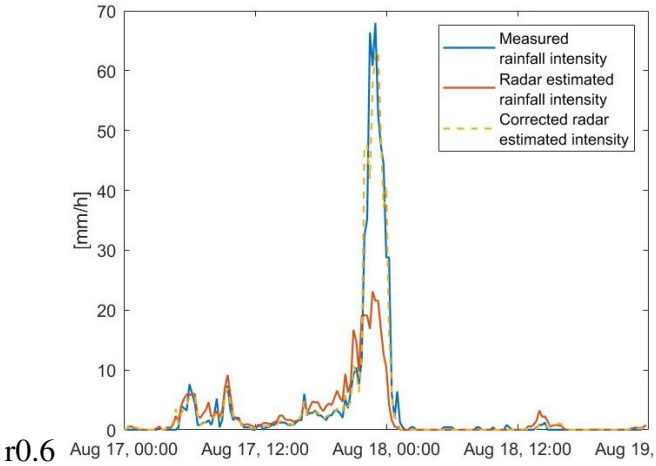

r0.6

Figure 4: The radar estimated (blue line), the station measured (orange line) and the corrected radar estimated rainfall intensity every 15 minutes. Based on data from SMHI (2021f).

both of the vectors the average relation between the radar estimated and the measured data was used instead. By using only non-zero values the correction factor will not become zero or go towards infinity. In other studies the limit is set so the data pair must exceed 1 mm/h to be valid (Goudenhoofdt & Delobbe 2009; Wardhana et al. 2017). The code used for correction of the radar estimated data against the measured data can be found in appendix A.1 and the corrected radar data in the position of the measurement station can be found in Figure 4.

3.3.3 Preparing precipitation input to the model

The rain event in Gävle on the 17th and 18th of August was rather long, and to make computational time reasonable, it is parted into a pre-rain and the actual simulation rain. The data from 2021-08-17 00:00 to 2021-08-17 20:00 is used as the pre-rain, which is simulated only once to give the saturation in the ground which is used as the initial water content in the ground for the rest of the simulations. This is based on the assumption that the rain intensity before 20:00 is not high enough to cause flooding, but will saturate the ground, reducing it's infiltration capacity when the intense part of the rain begins. Thereafter the data from 20:00 to 02:00 is simulated to investigate the hydraulic response in the model. The most intense part of the rain event take place 21:45- 00:45 with the peak intensity occurring between 23:00 and 00:00 in all the radar cells being in contact with the model area. The simulations are running at least 6 hours after the peak in every grid cell to include the peak response.

To create the precipitation input for the model the MFB-adjusted radar data from the real rain event were extracted as hyetographs with one hyetograph representing the rain over one specific radar grid cell of 2×2 km. There are 22 radar grid cells being in contact with some part of the model area. To correct for the stormwater system capacity, which is assumed to on average, over the whole area, be of a 5-year rain, the hyetographs were deduced by the intensity of a 5 year block rain with the same duration as the simulation rain. The intensity of a rain with a duration of 6 hours and a 5 year return period was calculated with Dahlström's formula (Equation 1) to be 5.6 mm/h and the deduction was made on every time step in the hyetographs, although the intensity never was allowed to

go below 0. Svenskt Vatten (2016) recommends the stormwater system to have the capacity of a 10 year rain in the central part of city, of a 5 year rain in densely built-up areas and of a 2 year rain in more sparesly built-up areas, but often the actual capacity is lower than this (MSB 2014). This is why a 5 year rain capacity is assumed for the model which are covering a large area including central, densely built-up and sparesly built-up areas. The duration of the deduction block rain was chosen to be the same as the rain duration.

These corrections were only applied to the part of the rain falling on hardened surfaces which are assumed to be connected to the stormwater system, in line with the assumptions made by MSB (2014). A grid with the different radar cells parted in hardened and non-hardened surfaces were created, georeferated and connected to the right hyetographs by assigning different identities to the different grid cells and different surfaces within the grid cells. This was together with the hyetographs connected to MIKE as the precipitation input.

To answer the research questions two uniform reference rains were created to compare the spatially varied radar estimation of the rain event with, and their hyetographs are presented in Figure 6. All the rain input files created are:

- **Pre-rain 00:00-20:00, from radar data:** A spatially varied rain with 22 hyetographs without a deduction connecting to the non-hardened surfaces in every grid cell and 22 hyetographs with a deduction for the stormwater system connecting to the hardened surfaces in every grid cell. The grid cells together with the outline of the model area can be seen in Figure 5a.
- **Rain event 20:00-02:00, from radar data:** A spatially varied rain with 22 hyetographs without a deduction connecting to the non-hardened surfaces in every grid cell and 22 hyetographs with a deduction for the stormwater system connecting to the hardened surfaces in every grid cell. The maximum intensity in the hyetographs varies over the area between 58 mm/h (cell 1) and 111 mm/h (cell 13) with an average maximum intensity of 87 mm/h, which can be seen in Figure 5a, and all the hyetographs connecting to the 22 cells can be seen in Figure 5.
- **Uniform with spatial mean hyetograph 20:00-02:00:** A spatially uniform rain with the spatial mean intensity from the 22 grid cells for every time step saved as one hyetograph, connecting to non-hardened surfaces, and the corresponding one with a deduction for the stormwater system connecting to hardened surfaces. This is to evaluate the effect of the spatial variability, so volume and duration are kept the same as in the spatially varied rain event. The average hyetograph together with the hyetographs it is based on can be seen in Figure 6.

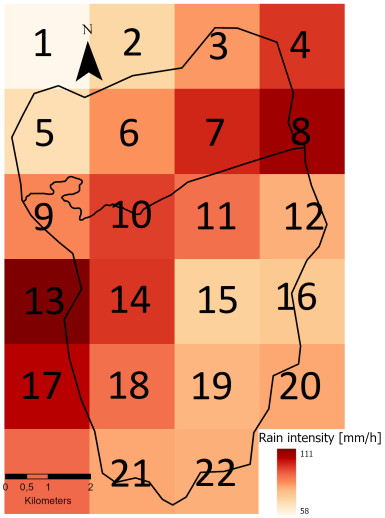

(a) Rain cells and the maximum intensity of their corresponding hyetographs

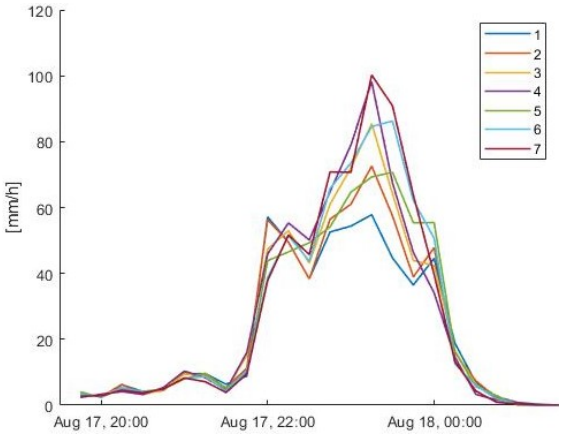

(b) Hyetographs for cell 1-7

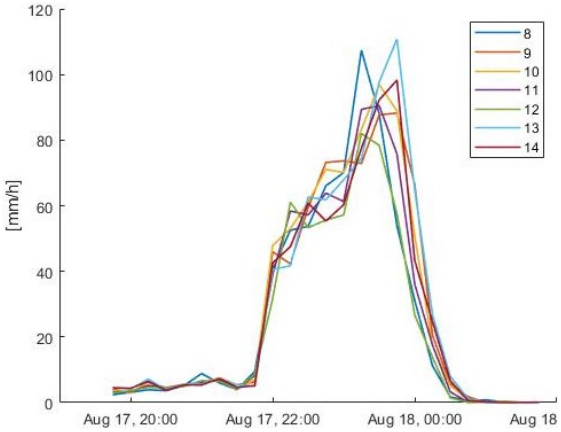

(c) Hyetographs for 8-14

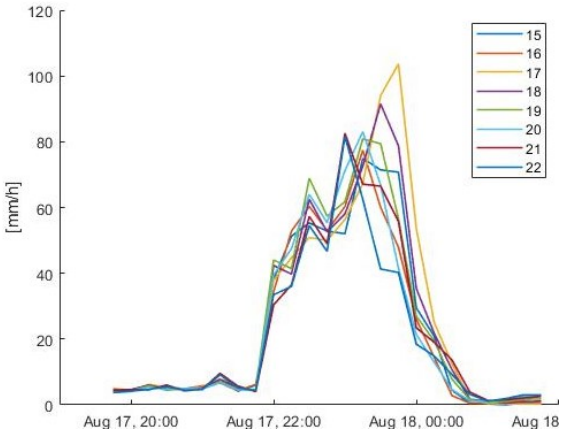

(d) Hyetographs for cell 15-22

Figure 5: The hyetographs for the spatially varied rain, without deduction, and the cells that they are connected to in the model area.

- **Uniform CDS with mean hyetograph volume:** A spatially uniform CDS rain with the same volume and duration as the spatial mean hyetograph rain, i.e. 155 mm in 6 hours, connected to non-hardened surfaces and a corresponding one with a deduction for the stormwater system connected to the hardened surfaces. This is to evaluate the effect of a CDS temporal variation which is common practice to use in cloudburst modelling, often with a duration of 6 hours. The CDS hyetograph was generated with a program provided by Tyréns with r-parameter, i.e. the part of the rain occurring before the peak, chosen to be 0.37, which is common practice in creation of CDS design storms, and within the range recommended by Arnell (1982). The CDS hyetograph with the same total volume as the average hyetograph can be seen in Figure 6.

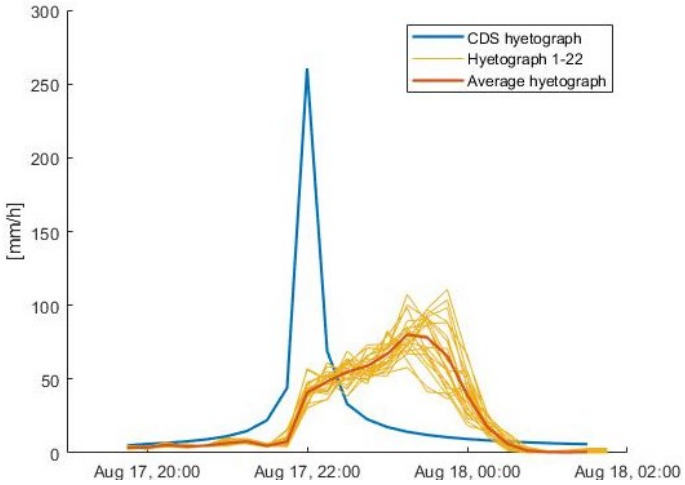

Figure 6: Average hyetograph (orange) from the Gävle cloudburst and a CDS hyetograph (blue) with the same total volume. The hyetographs the average is based on are also included in yellow.

3.4 Evaluation of scenarios

The simulations gave results in the form of flooding depth for every time step over the whole model area and a maximum flooding depth over the whole model. The results for the whole model area is not of interest for the study however, and not valid since resolution is very coarse in rural parts, which are included only to correctly describe the flow and flooding in the central part of the model. A central part of the model was chosen for evaluation, and the borders of this part were chosen based on the area having the highest resolution, of maximum 4 m^2 per element, which can be seen in Figure 3, but extend a bit westwards to include parts later assessed as central. The influence from the spatial variation of the rain intensity was studied by comparing how large part of the area that was flooded and the average maximum flooding depth in the area for the different rain scenarios, which is the deepest flooding depth in each of the model elements registered at any time during the simulation, spatially averaged over the evaluation area, which is the central model area.

To get an estimation of how well the model performed, validation data was searched for in the form of photos and measurements from the Gävle cloudburst and compared with the simulated flooding depth from the spatially varied rain, which is assumed to be the best estimation of the actual rain event in this study, and with the two uniform rain scenarios. The evaluation points were chosen based on where measurements or photos for validation of the model were available, but also with an aim to evaluate the flooding in different parts of the central model area.

Flooding statistics for every simulation were studied in MIKE Zero where information of number of elements in the model and the average maximum depth could be derived directly with the tool *calculate statistics*. 0.1 m was chosen as the limit for an area being counted as flooded in the analysis of the results. This flooding depth is not the same as the flooding depth parameter used as an input for MIKE (0.01 m), which is only needed to define if an element is to be included in the calculation of the fluxes. With the tool *select values* the number of elements reaching a maximum water depth of 0.1 m or higher could

be derived and then divided by the total number of elements to get the part of the area being flooded. Flooding statistics were derived for the part of the model area counted as central through loading a shape-file with the outline of the central part in MIKE Zero and selecting the elements being within the central part, which was saved as a selection and used for all scenarios.

To get an overview of the simulated flooded depth from the spatially varied rain, that is thought to represent the actual cloudburst, a map showing the maximum flooding depth from this simulation was produced in ArcGIS. This was also used to mark the positions of the validation points. The difference between the spatially varied rain and the two uniform scenarios were mapped using the ArcGIS tool *calculate raster*, creating a raster with the difference in flooding depth between the uniform and varied rain in cm calculated as $D_{Umax} - D_{Smax}$ and in percent according to Equation 4. D is flooding depth and D_{Umax} represents the maximum flooding depth from the uniform rain in meters, D_{Smax} the maximum flooding depth from the spatially varied rain in meters, and the difference, ΔD, is given as percent of the varied rain, with a negative value indicating that the uniform rain is underestimating the flooding compared to the spatially varied rain and vice versa.

$$\Delta D = \frac{D_{Umax} - D_{Smax}}{D_{Smax}} \cdot 100 \tag{4}$$

Figures showing the flooding depth difference in only the central part of the model area and in only the areas counted as flooded by the spatial rain, i.e. reaching a maximum flooding depth of at least 0.1 m, were also produced. This gives a better view of the most interesting parts; excluding the parts with a flooding depth $<$0.1 m is also relevant since a relative difference can become very high if the flooding depth is low. The part of the area being flooded by the spatially varied rain were extracted with the tool *extract by attributes* in ArcGIS and this raster could then be used to cut out same areas in the other rasters with the tool *extract by mask*. To quantify the difference between the uniform and spatial scenarios in the flooded central parts of the model and get a perception of the uncertainty that the uniform rains might have, rasters with the absolute difference [m], relative difference [%] and absolute values of the absolute and relative differences of the flooding depth were created for both the uniform scenarios with the tool *raster calculator* and the mean values of these were derived from the statistics available in the properties for a raster. The spatial average of the absolute value of the difference in flooding depth between the uniform and the spatially varied scenarios is thought to give the most clear quantification of the uncertainty in the results from the simulations with uniform rains, if the spatially varied rain is assumed to generate the real flooding depth. This is derived for the flooded central parts of the model since these are of the highest interest. The average of the absolute value of the difference, $\mid \Delta D \mid$, is derived according to Equation 5, where D_{Umax} and D_{Smax} are cut to only include the central model area flooded by the spatially varied rain.

$$\mid \Delta D \mid = \text{mean} \left(\frac{\mid D_{Umax} - D_{Smax} \mid}{D_{Smax}} \cdot 100 \right) \tag{5}$$

4 RESULTS

4.1 Flooding from spatially varied rain event

The maximum flooding depth from the spatially varied rain, based on radar data, in the whole model area is presented in Figure 7 where all areas reaching a maximum flooding depth of at least 0.1 m are marked with a color from blue to red depending on the flooding depth. Many streets in the central parts of the city can be seen as blue, i.e. with a flooding depth of 0.1-0.4 m. At some viaducts the flooding depth can be seen to reach above 2 m, and in certain areas such as the southern allotment garden area the flooding depth reaches above 1 m. The central part of the model mainly used for evaluation is marked with a black outline.

4.1.1 Validation

A validation of the model with the spatially varied rain, which aims to represent the real rain event, is performed by comparing the simulated flooding depth in different points with information derived from photos or measurements. The real flooding depth, measured or estimated from photos, can be seen in Table 5 together with the simulated flooding depth at the same point and on the same time. In the cases where the estimation is of the maximum flooding depth, this is what is given in the column for the simulated depth as well. The difference between the simulated and actual depth is also given as percent of the actual flooding depth. To give some insight of how precise or imprecise the estimation of the actual flooding depth is for that point a comment on what the validation data is based on is also presented in the table and for the two more imprecise validation points the estimated real depth is given as a range instead as a value. The positions of the points are marked in Figure 7 together with the maximum flooding depth from the spatially varied rain.

Table 5: Validation data in 7 evaluation points from measurements and photos and simulated flooding depth from the spatially varied rain

Point Coordinate (SWEREF99 TM)	**Estimated real depth**	**Time of photo/ measurement**	**Simulated depth**	**Difference as % of real depth**
1 House in Hemingby 618109, 6726169	1.06 m	At maximum	1.07 m	0.9%
	Based on measurement on facade of a house			
2 Allotment garden 618442, 6727092	0.85 m	7:55	0.82 m	3.5%
	Based on photo with water reaching up to window and measurement			
3 Hemsta roundabout 618339, 6726647	2.45 m	7:54	2.37 m	3.3%
	Based on photos of viaduct, water level on petrol station and DEM			
4 Coop Brynäs 619329, 6727913	0.49 m	10:12	0.51 m	4.1%
	Based on photo of parking area from above and DEM			
5 Viaduct Strömsbrovägen 617591, 6729141	2.87 m	10:30	2.92 m	1.7%
	Based on photo from the viaduct and DEM			
6 Viaduct Norra Kungsgatan 616750, 6729244	2.70-3.00 m	At maximum	3.03 m	1-12%
	Based on observations of water going up to a nearby roundabout and DEM			
7 Campus 615564, 6727735	0.3-0.45 m	8:00	0.43 m	4-43%
	Based on photo with water reaching almost up to the knees of two persons and standard height of knees			

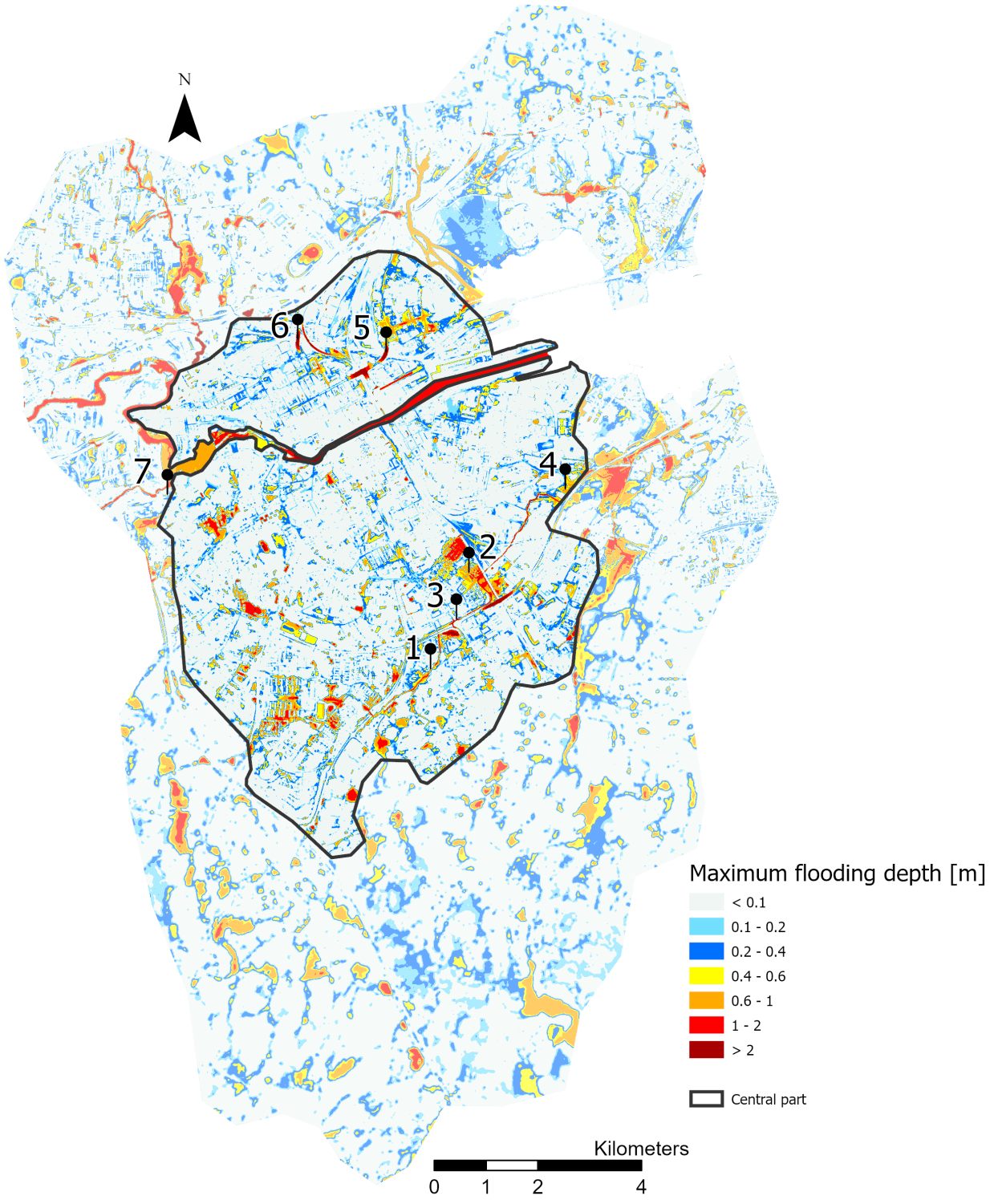

Figure 7: The maximum flooding depth of the spatially varied rain given in meters and the position of the evaluation points. The central part of the model area is marked with a black outline.

In Table 6 the validation data is presented together with the flooding depth in the same point in time and space for all the three rain scenarios together with the difference from the estimated actual flooding depth. For the five more precise validation points, 1-5, an average of the difference in flooding depth is presented for the three rain scenarios and

they are all within 2.7-4.2% from the estimated actual flooding depth, with the spatially varied rain being closest with 2.7%.

Table 6: Validation data in 7 evaluation points from measurements and photos compared with the flooding depth from the rain scenarios at the same point in time and space

Point	**Estimated real depth**	**Simulated flooding depth (difference in % from real depth)**		
		Spatially varied	Uniform mean hyetograph	Uniform CDS hyetograph
1	1.06 m	1.07 m (0.9%)	1.08 m (1.9%)	1.05 m (0.9%)
2	0.85 m	0.82 m (3.5%)	0.81 m (4.7%)	0.82 m (3.5 %)
3	2.45 m	2.37 m (3.3%)	2.34 m (4.5%)	2.35 m (4.1%)
4	0.49 m	0.51 m (4.1%)	0.53 m (8.2%)	0.53 m (8.2%)
5	2.87 m	2.92 m (1.7%)	2.92 m (1.7%)	2.92 m (1.7%)
Average difference for point 1-5	-	2.7%	4.2%	3.7%
6	2.70-3.00 m	3.03 m (0-12%)	2.98 m (0-10%)	2.94 m (0-9%)
7	0.3-0.45 m	0.43 m (0-43%)	0.40 m (0-33%)	0.40 m (0-33%)

4.2 Flooding statistics for different rain scenarios

Statistics of the maximum flooding depth were derived from every simulation and from this the average maximum flooding depth was derived for the central area, including both flooded and non-flooded elements. An element was chosen to be called flooded when the water depth was equal to or greater than 0.1 m and the part of area flooded was investigated by calculating the fraction of the model elements that reached a water level of 0.1 m at any time of the simulation. The part of model area being flooded and the average maximum flooding depth are presented in Table 7 for the different rain scenarios in the central part of the model, and the part of the central area reaching different maximum flooding depths are visualised in Figure 8. The area counted as central can be seen in Figure 7.

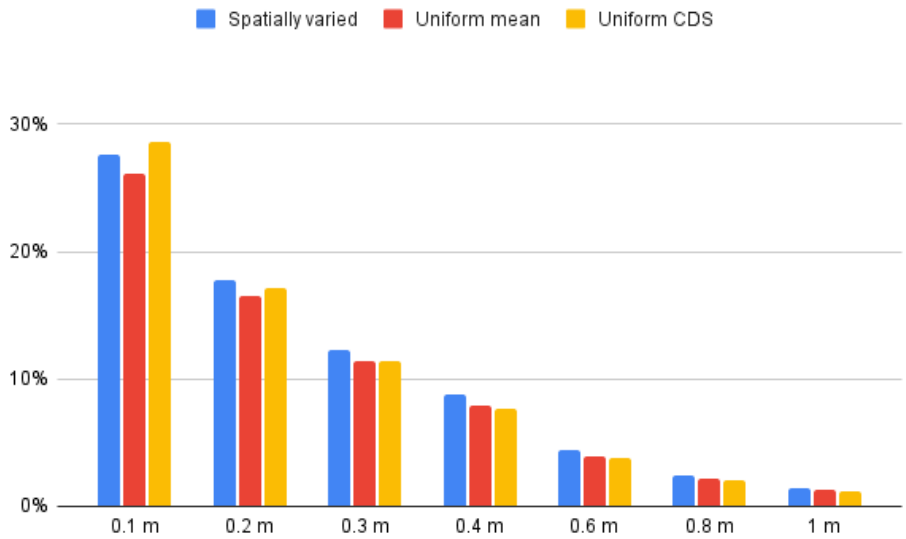

Figure 8: Part of the central area reaching different maximum flooding depths for the three scenarios.

The average maximum flooding depth is the highest for the spatially varied rain and varied by 3 to 6% between the scenarios in the central part of the model, with a maximum of

6% difference between the spatially varied rain and the uniform with mean hyetograph. The part of the area being flooded varies by up to 10% between the scenarios, where the largest proportion of the area being flooded is for the uniform CDS rain. The uniform rain with the mean hyetograph gives a smaller proportion of the central area flooded, -6%, compared to the spatially varied rain, while the uniform CDS gives a 4% larger proportion of the area that is flooded.

Table 7: Statistics of the hydraulic response from the simulation of the different rain scenarios in the central part of the model area, including non-flooded areas

Rain scenario	**Part of area flooded**		
	Central part	Difference from spatial	Difference from mean hyetograph
Spatially varied	27.6%	-	
Uniform mean hyetograph	26.1%	-6%	-
Uniform CDS hyetograph	28.6%	+4%	+10%
Rain scenario	**Average maximum flooding depth**		
	Central part	Difference from spatial	Difference from mean hyetograph
Spatially varied	12.5 cm	-	
Uniform mean hyetograph	11.7 cm	-6%	-
Uniform CDS hyetograph	12.1 cm	-3%	+3%

Statistics of the flooding difference between the uniform scenarios and the spatially varied one, with only the flooded areas of the central part of the model included, can be seen in Table 8. Statistics included in the analysis are the average of the relative difference in % of the flooding depth from the spatially varied rain and the average of the absolute values of the absolute [cm] and relative [%] difference. From the table it can be read that both the uniform rains on average have a lower flooding depth than the spatially varied rain. The uniform CDS have an average maximum flooding depth closer to the spatially varied one (-9%) compared to the uniform mean hyetograph rain (-12%), but the average of the absolute values of the difference shows that it varies more, by 15.7% compared to 10.9%. The central and flooded part of the model area, which the analysis is done for, can be seen in Figure 7 as the part being within the black outline and having another color than light grey, i.e. reaching a maximum flooding depth higher than 0.1 m by the spatially varied rain.

Table 8: Statistics of the difference and absolute value of the difference (|difference|) in maximum flooding depths between the uniform scenarios and the spatially varied one in the central and flooded (depth >0.1 m) part of the model area

Rain scenario	**Average difference from spatial in central flooded area**		
	Difference	| Difference |	| Difference |
Uniform mean hyetograph	-12%	7.8 cm	10.9%
Uniform CDS hyetograph	-9%	9.1 cm	15.7%

4.3 Uniform with spatial mean hyetograph

The difference in maximum flooding depth between the spatially varied rain and the uniform rain with the spatial mean intensity is presented in Figure 9 as percent of the maximum flooding depth of the spatially varied rain. Where the color in the figure is blue

the uniform rain is underestimating the flooding depth and where the colour is yellow to red in the figure it is overestimating the flooding, compared to the spatially varied rain. The maximum flooding depth from the uniform mean hyetograph rain used to derive the difference can be found in Appendix A.3 Figure A.1 .

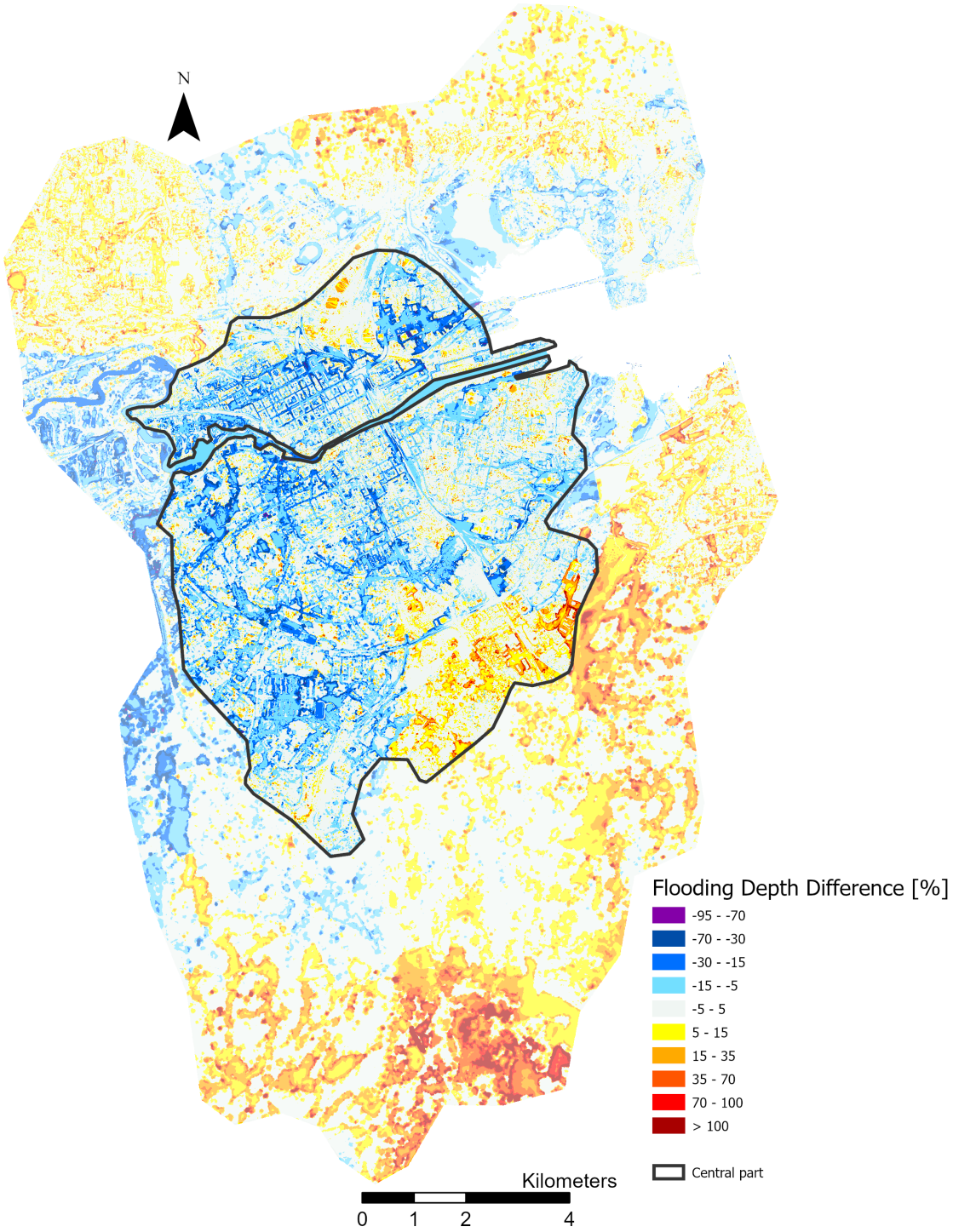

Figure 9: Difference in flooding depth derived by subtracting maximum flooding depth of the spatially varied rain from the maximum flooding depth of the uniform rain with mean hyetograph for the model area. The difference is given in percent of the maximum flooding depth from the spatially varied rain.

The uniform rain can be seen to underestimate the flooding depth compared to the spatially varied rain by 5-35% in most of the streets in the central parts of the model area, marked with a black outline in Figure 9 and viewed more easily in the zoomed in Figure 10. In the northwestern part of the model area, Sätra, the uniform rain is instead seen to slightly overestimate the flooding depth, generally by 5-15% (Figure 9). This is also the case for the southern and more rural parts of the model area were flooding depths in some places are overestimated by up to over 100%.

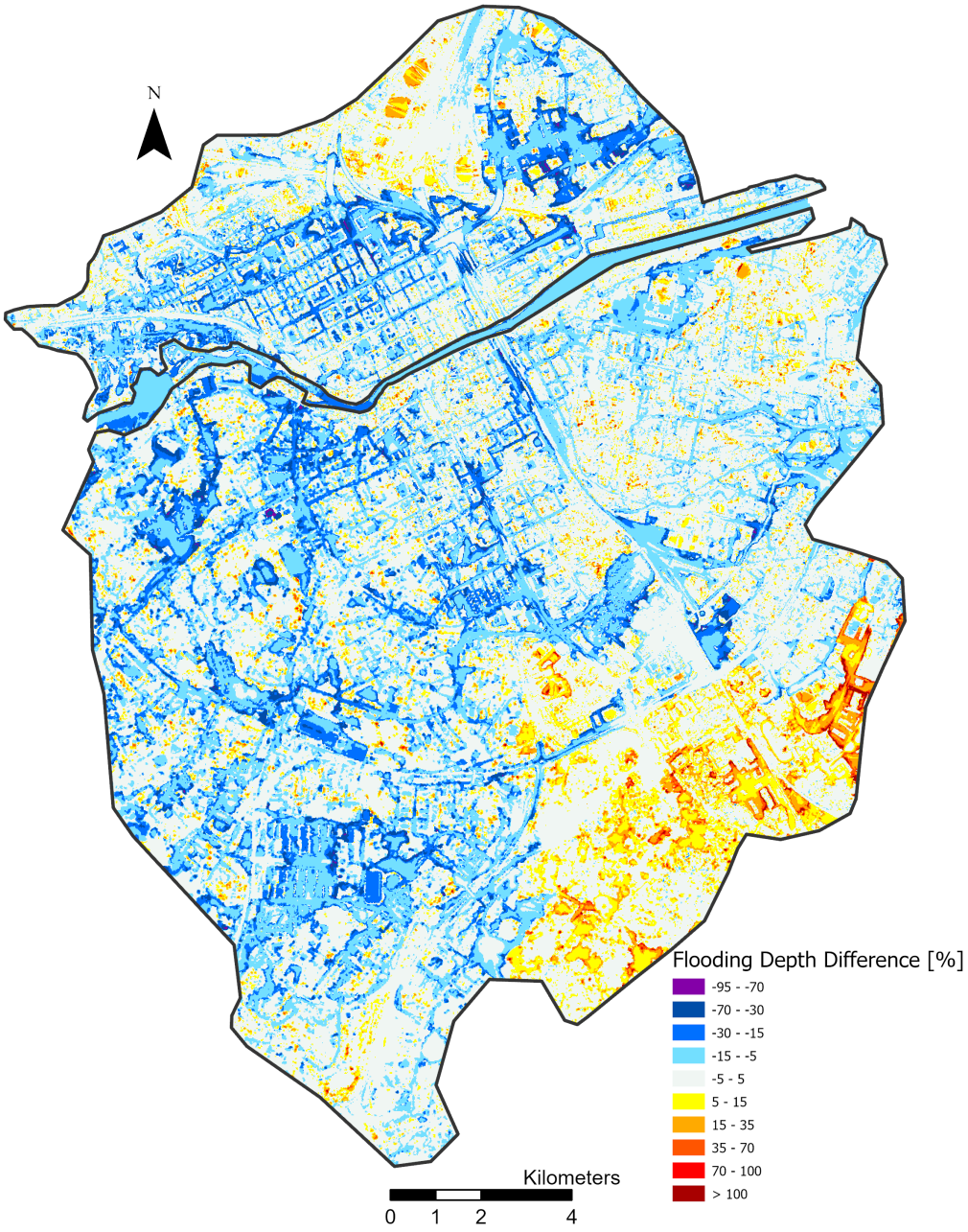

Figure 10: Difference in flooding depth in the central parts of the model area derived by subtracting maximum flooding depth of the spatially varied rain from the maximum flooding depth of the uniform rain with mean hyetograph. The difference is given in percent of the maximum flooding depth from the spatially varied rain.

The relative difference in flooding depth can be large for an area with a low flooding depth, even though the absolute difference is small. Therefore the relative difference in

flooding depth derived only for areas reaching a maximum depth of at least 0.1 m from the spatially varied rain, i.e. counted as flooded, is showed in Figure 11, other areas are white. In this figure it can be seen that in most of the flooded parts of the central model area the uniform rain is underestimating the flooding depth by 5-35%, except for some parts in the southeast where an overestimation by 5-35% can be seen. The spatial average of the difference from the spatially varied rain in the central flooded part is -12% and the average of the absolute value of the difference was calculated to 10.9% (Table 8).

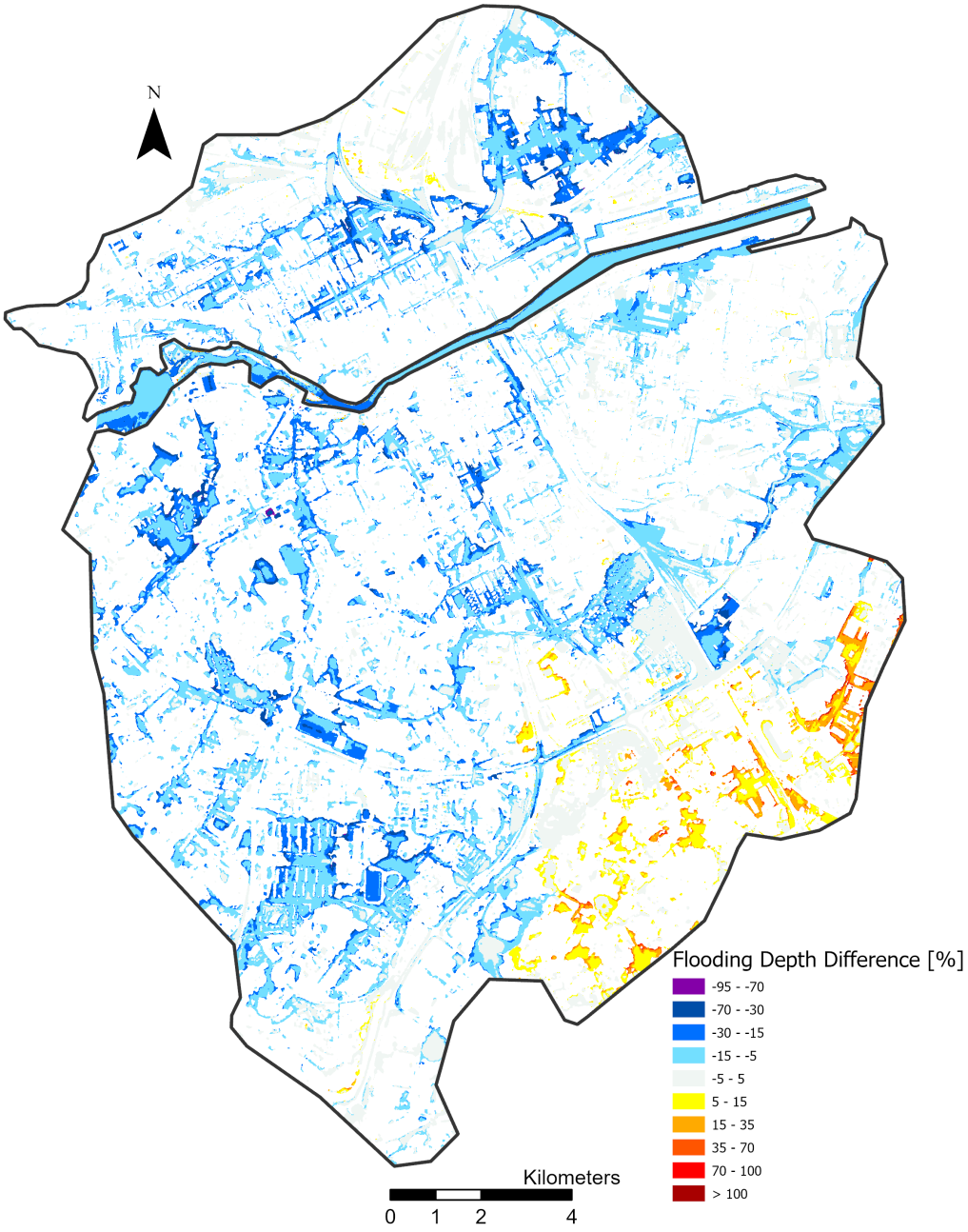

Figure 11: Difference in flooding depth in the central parts of the model area, with only the parts reaching a maximum flooding depth of at least 0.1 m included. Difference is derived by subtracting maximum flooding depth of the spatially varied rain from the maximum flooding depth of the uniform rain with mean hyetograph. The difference is given in percent of the maximum flooding depth from the spatially varied rain.

The absolute flooding depth difference given in cm for the central area can be seen in Figure 12, and a figure showing the absolute difference for the full model area can be found in Appendix A.4. In the central parts of the model area the uniform rain with a mean hyetograph is seen to generally give a 3-15 cm lower flooding depth (seen as blue in the figure) compared to the spatially varied rain, studying the areas where the difference is larger than 3 cm, other areas are seen as grey in the figure. On average the maximum flooding depth from the uniform rain with a mean hyetograph in the whole central part is 11.7 cm, where the spatially varied rain produces an average maximum flooding depth of 12.5 cm.

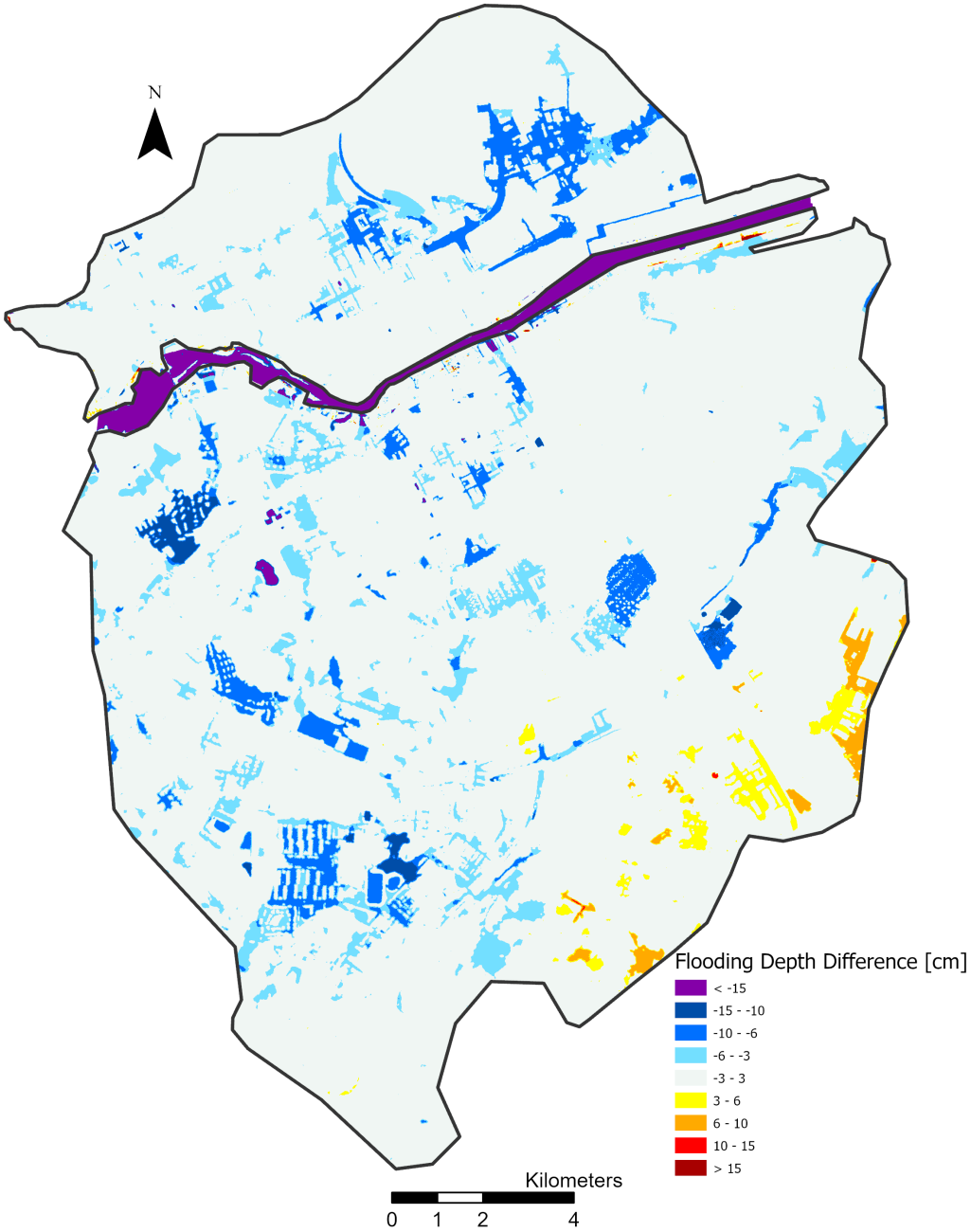

Figure 12: The flooding depth difference in the central area between the uniform rain with a mean hyetograph and the spatially varied rain given in centimeters. Calculated by subtracting flooding depth by uniform rain from flooding depth by spatial rain.

4.4 Uniform with CDS hyetograph

The difference in flooding depth between the uniform CDS rain and the spatially varied rain as percent of the spatially varied rain is shown in Figure 13.

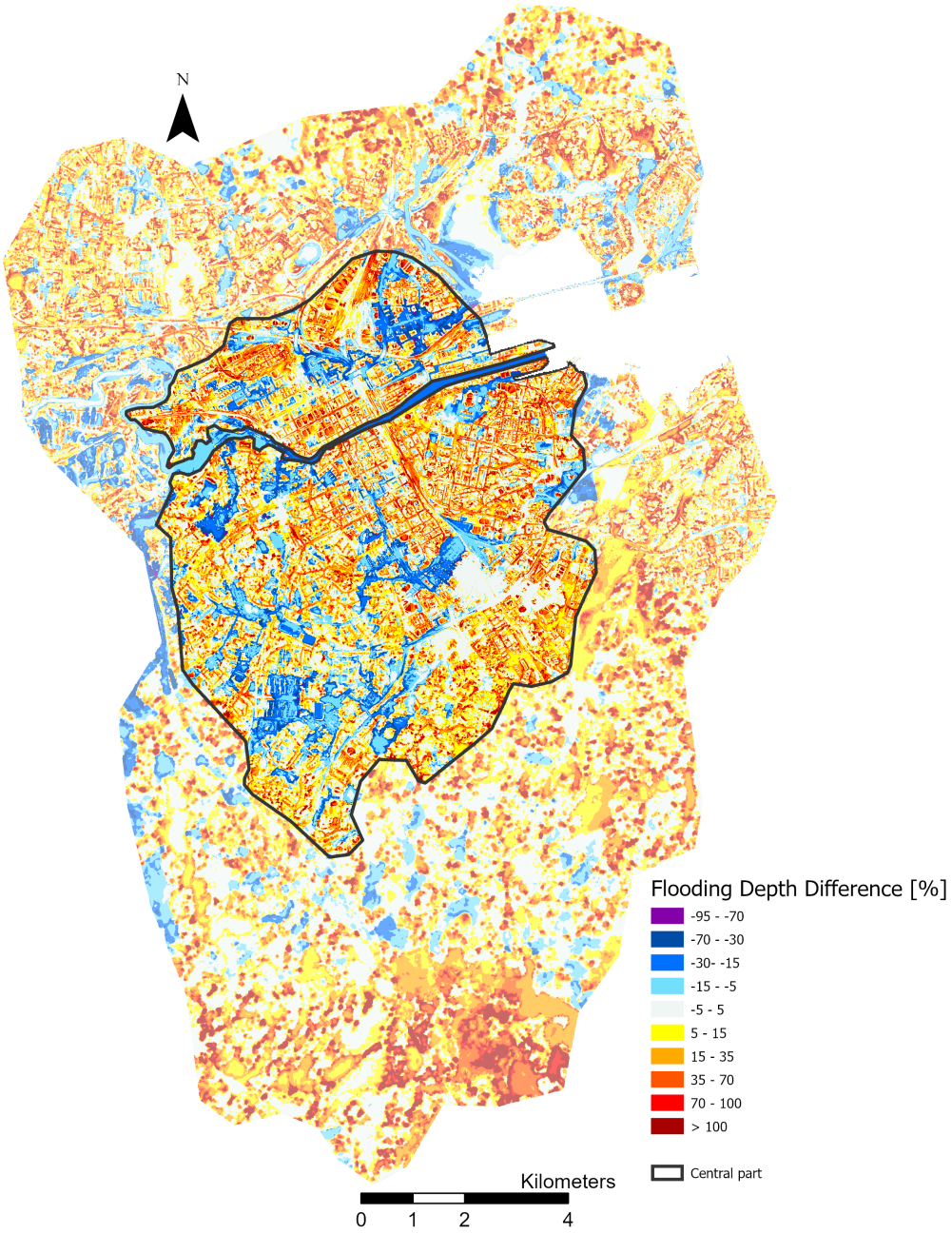

Figure 13: Difference in flooding depth derived by subtracting maximum flooding depth of the spatially varied rain from the maximum flooding depth of the uniform rain with CDS hyetograph for the model area. The difference is given in percent of the maximum flooding depth from the spatially varied rain.

In the blue areas of Figure 13 the uniform CDS rain is underestimating the flooding depth compared to the spatially varied rain and where the color in the figure is yellow to red the uniform rain is overestimating the flooding depth. The difference in flooding depth can be seen to vary largely over the model area with positive and negative differences occurring in all parts of the model area. The maximum flooding depth from the uniform CDS rain used to derive the difference can be found in Appendix Figure 13.

Figure 14 is showing the difference in flooding depth between the uniform CDS rain and spatially varied rain in the central part of the model area only, which is the area of interest for evaluation. In this figure the uniform CDS is seen to overestimate the flooding depth in parts of the central area by up to and over 100% in many places(seen as red in the figure), but also with several parts in blue where the CDS underestimates the flooding depth relative to the spatial rain.

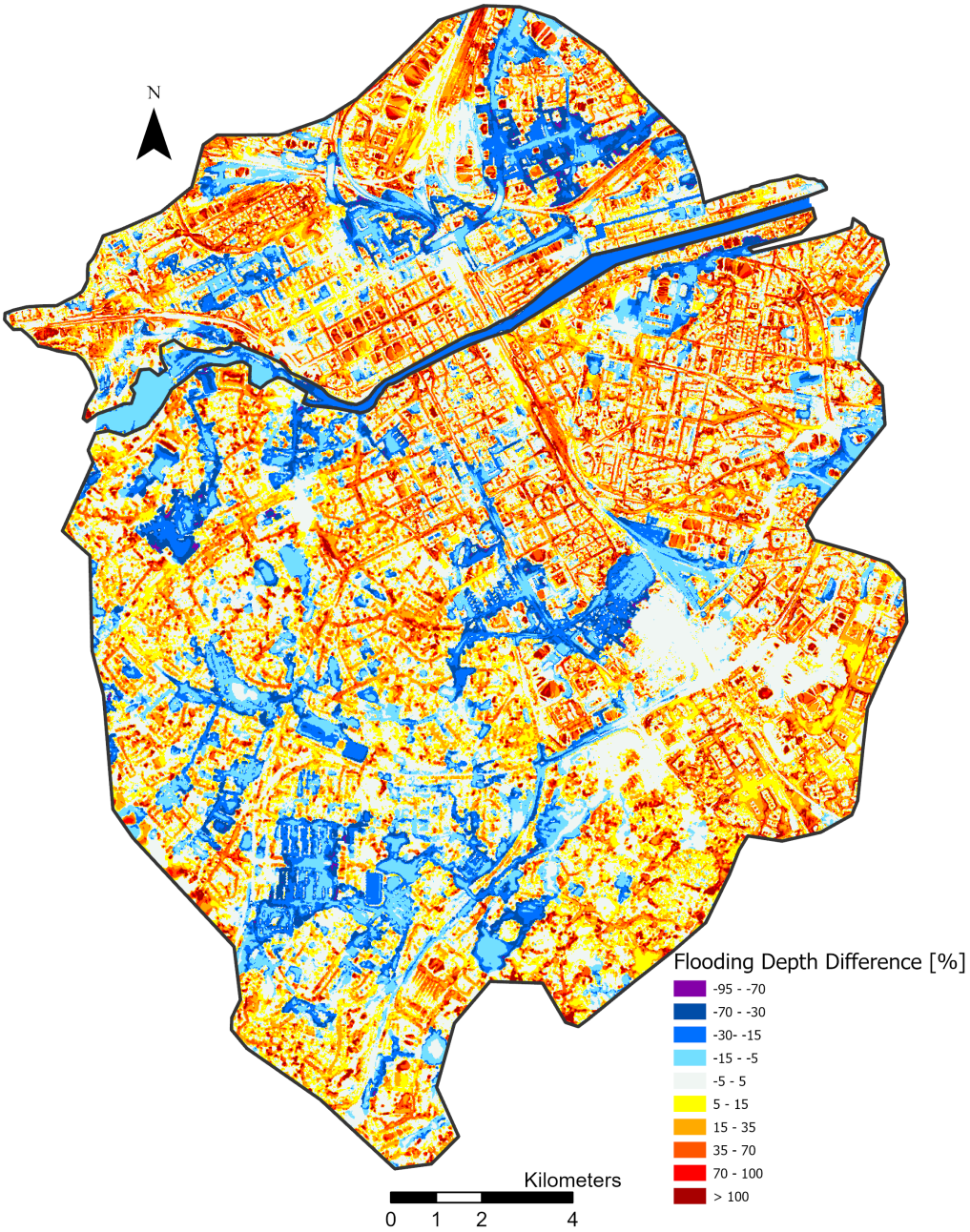

Figure 14: Difference in flooding depth in the central parts of the model area derived by subtracting maximum flooding depth of the spatially varied rain from the maximum flooding depth of the uniform CDS rain. The difference is given in percent of the maximum flooding depth from the spatially varied rain.

Figure 15 is showing the flooding depth difference between the uniform CDS and the spa-

tial rain for the central part of the model, but only for the areas that is counted as flooded by the spatially varied rain (reaching a maximum flooding depth of at least 0.1 m), other areas are white. This figure shows that in flooded areas the uniform CDS is generally underestimating the flooding depth, since larger parts of the central area that is included is blue compared to yellow to red. The spatial average of the difference from the spatially varied rain is -9% in the central flooded part and the average of the absolute value of the difference in this part was calculated to 15.7% (Table 8).

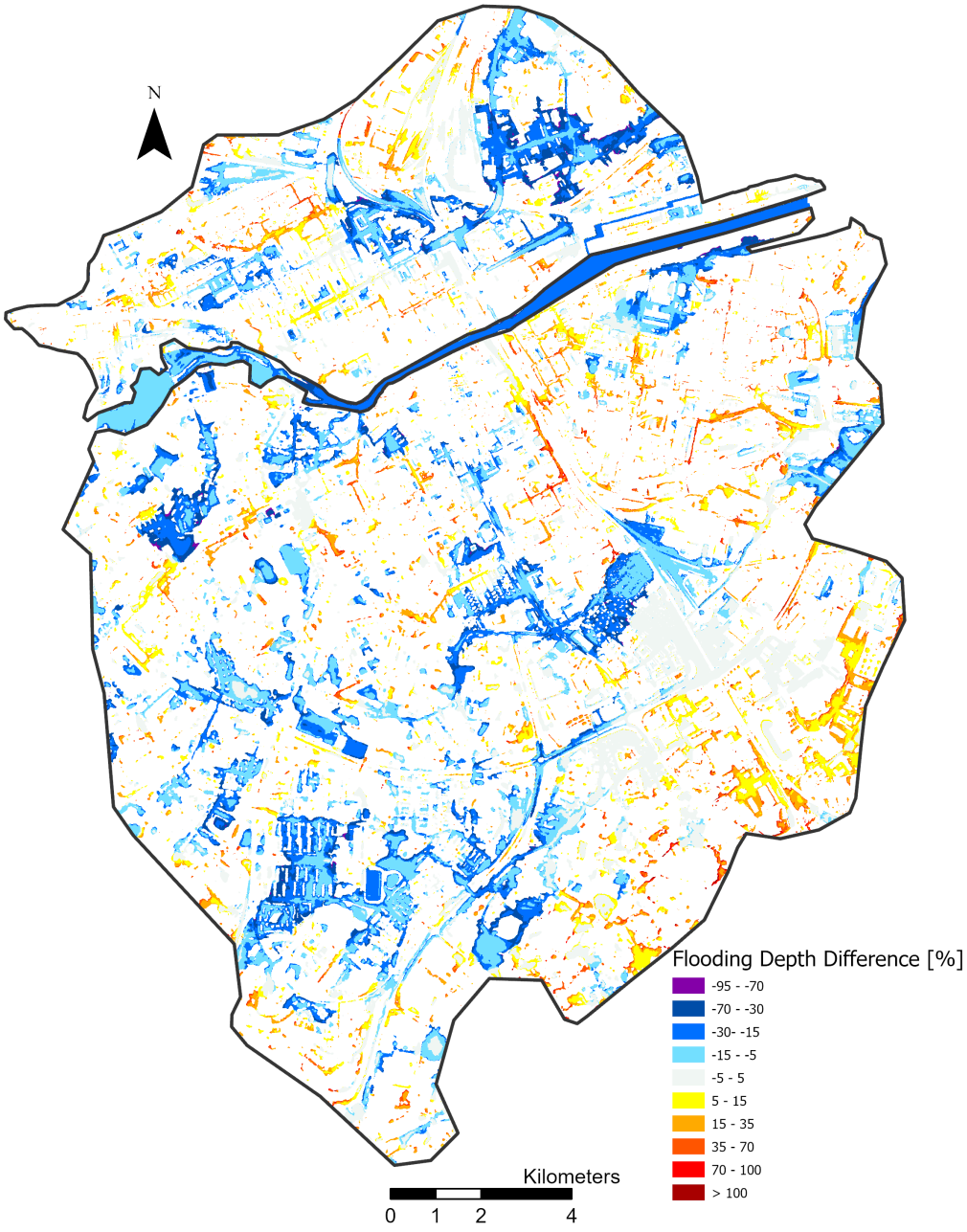

Figure 15: Difference in flooding depth in the central parts of the model area, with only the parts reaching a maximum flooding depth of at least 0.1 m included. Difference is derived by subtracting maximum flooding depth of the spatially varied rain from the maximum flooding depth of the uniform CDS rain. The difference is given in percent of the maximum flooding depth from the spatially varied rain.

The absolute flooding depth difference given in cm for the central area can be seen in

Figure 16, and a figure showing the absolute difference for the full model area can be found in Appendix A.4. In the central parts of the model area the uniform CDS rain is seen to both give a lower and higher flooding depth compared to the spatially varied rain in the areas with a difference larger than 3 cm. On average the maximum flooding depth from the uniform CDS rain in the whole central part is 12.1 cm, which is lower than from the spatially varied rain which produces a maximum flooding depth of 12.5 cm.

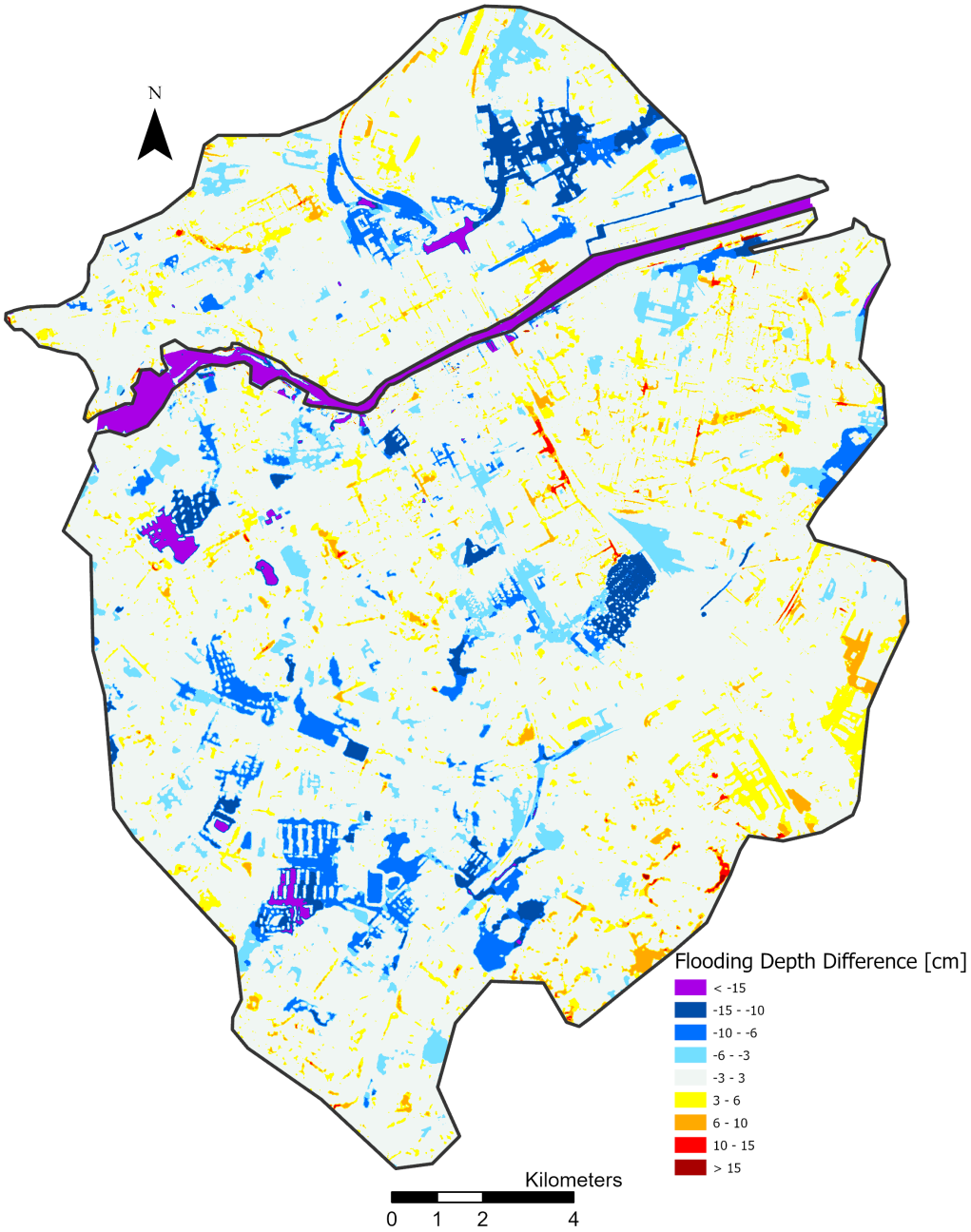

Figure 16: The flooding depth difference in the central area between the uniform rain with a CDS hyetograph and the spatially varied rain given in centimeters. Calculated by subtracting flooding depth by uniform rain from flooding depth by spatial rain.

5 DISCUSSION

This section will start by commenting the most important aspects of the model inputs and how these can have affected the results and then move on to validation of the model, which aims to find if the model inputs and different assumptions made were good enough for the model to represent the reality well. Lastly the actual results and larger aims of this project of how the spatial variations of intense rains and the common practice of using uniform CDS design storms affect modelled hydraulic response will be discussed in subsection 5.4 and 5.5.

5.1 Precipitation input

5.1.1 Calibration of radar data

The radar estimated rainfall intensity was calibrated against rainfall data from the Gävle measurement station hold by SMHI. Calibration of radar data is usually needed, since it often lacks in accuracy due to this being an indirect method, deriving rain intensity from reflectivity measurements (Goudenhoofdt & Delobbe 2009; Ochoa-Rodriguez et al. 2019). Rain gauges however usually have a good accuracy, but can only describe the point rainfall and radar data is a good complement to capture the rainfall's spatial variability. Studying the station measured rainfall intensity from the Gävle cloudburst and the radar estimated rainfall intensity at the station's location (Figure 4) one can see that some kind of bias is affecting the radar data and it was concluded that a calibration is needed.

The method used in this study is a hourly mean field bias adjustment, which assumes that there is a spatially uniform but temporally varied multiplicative error in the radar estimation of the rain intensity, that can be adjusted by multiplying the radar data from the whole area with a temporally varied factor. This method was chosen since it was supported and used by many other studies, but still simple (Q. Qiu et al. 2020; Smith & Krajewski 1991; Thorndahl et al. 2014; Wardhana et al. 2017). This method assumes that the rain gauge at the measuring station is giving the correct rainfall intensity, which of course is not entirely true since all measuring methods have their weaknesses, for example wind can cause problems in catching all the rainfall in the rain gauge and act as a source of error. The measurements is the best available estimation of the true rainfall though, and was thus assumed to be the correct rainfall.

There are also spatially varied correction methods creating a calibration field instead of a vector, such as Static local bias correction (SRD) or Brandes spatial adjustment (BRA), which both have a correction factor being a function of the distance to different rain gauges in the radar field (Goudenhoofdt & Delobbe 2009). Then there are also kriging methods, creating a radar based kriging field from radar values at different gauge sites, used to obtain an error field (Goudenhoofdt & Delobbe 2009; Ochoa-Rodriguez et al. 2019). Using correction methods like these was not relevant in the Gävle case since only one rain gauge measurement was available. Having a spatially uniform radar correction is a simplification, but this have shown to give sufficiently good results in other cases. In the Gävle case, with only one rain gauge available in the area, this seemed to be the most reasonable choice.

5.1.2 Deduction made for the stormwater system

The stormwater system can be taken into account in many different ways. Including the stormwater system as a 1D-model, which would be the most accurate, was not possible within the time frame of this project and with the available information, therefore the capacity of the stormwater system was instead accounted for as a deduction of the precipitation input. This is the recommended method by MSB (2014) for scenarios with high intensity rainfall, cloudbursts, since the stormwater system capacity in these cases are very small compared to the rainfall intensity, and uncertainties in the deduction will therefore only have a small impact on the results. The deduction made in this case is by the intensity of a 5 year block rain with a 6 hour duration. The capacity of the stormwater system in Gävle was not known so the deduction is based on an estimation and on recommendations. Stormwater systems are recommended to have the capacity to handle a 2 to 10 year rain, depending on how central the urban area is (Svenskt Vatten 2016). The real capacity is however often lower than the recommended ones (MSB 2014), and there is also a risk for waste clogging the pipes when a cloudburst is flushing the streets, decreasing the capacity. A simplification was made by applying the same stormwater system deduction over the hardened surfaces in the whole model area in this study, and therefore the capacity was chosen to be of a 5 year rain with a 6 hour duration, same as the simulation rain duration. This is probably an underestimation at least in central parts of the city, but can also be reasonable if the pipes are already partly filled from previous raining and some pipes might have reduced capacity due to clogging or other reasons. This estimation is very uncertain, but it will likely not overestimate the stormwater system capacity. The stormwater system capacity should be rather small in relation to a rain with the intensity of the Gävle cloudburst in August, which for comparison has a return period of 660 years using the Dahlström formula and a 6 hour duration. Which means that the estimation of the stormwater system capacity is less important than in a case with a rain of lower intensity. Therefore the error introduced by the uncertain deduction for the stormwater system is assumed to not affect the results largely. The return period of the rain event is mentioned to be put in relation to the recommended dimensioning rains of the stormwater system, but it should also be said that the Dahlström formula is not very suitable for calculating rain events of this low frequency, since the statistical basis naturally is very weak for this.

5.1.3 The spatial resolution of the radar data

The radar data produced by SMHI which is used in this study have a spatial resolution of 2×2 km with the rain intensity being spatially averaged within these cells. This is a rather rough resolution considering conclusions from studies on the spatial variation of rainfall intensity presented in section 2.5. For example Goodrich et al. (1995) finding that rainfall depth varied by 4-14% between measuring points only 100 m apart and Fiener & Auerswald (2009) observing a variation of on average 4.2 mm/km, concluding that the assumption of a spatially uniform rainfall is invalid even at a sub-kilometer scale. Several studies presented in section 2.5 also pointed out that the spatial variability was higher for more intense rainfall, which implies that the radar is likely to have smoothed out some intensity peaks from the Gävle cloudburst by spatially averaging over one 4 km^2 radar cell. If a peak occurred in a sensitive area giving a direct hydraulic response this response will be overlooked by the model. This means that the actual difference between a real and

intense rain event and a uniform design storm of the same volume might be larger than the results this study is showing, based on literature presented in section 2.5. A finer resolution of the radar would have been preferable to simulate an intense rainfall. To use a finer resolution in modelling does increase computational time though, and it might therefore be relevant to use a rougher resolution if it produces acceptable results.

The spatial resolution is also affecting the average hyetograph produced in this study since all radar cells being in contact with the model area are included in the averaging, without spatially weighting for how large parts of the radar cells that is included. The resolution of the uniform rainfall is also dependent on the model area size. The difference between the uniform and spatially varied rain should be smaller in a smaller model area where the uniform design storm would be closer to a spatially varied one in resolution, and the difference in hydraulic response should be less. In this case, the full model area is 54 km^2 and the uniform rains can be said to have the resolution of 54 km^2 compared to the 4 km^2 resolution of the spatially varied rain.

5.2 Other model inputs

The spatially varied model input, which is bed resistance and infiltration, is simplified to only differentiate between hardened and non-hardened surfaces. To make this more detailed, basing it on land use and soil type maps, and assign different surfaces with different Manning numbers and infiltration rates would have been a more precise but also more time consuming approach. In urban areas filling material or topsoil is often added to the top layer of the ground, and the actual infiltration capacity can differ from the theoretical capacity for that soil type (MSB 2017). This uncertainty of the actual surface material, lack of information on infiltration rates for different materials and an aim to find simplifications to reduce the time demanded to prepare the model led to the decision to only differentiate between hardened and non-hardened surfaces. This is the most important differentiation and is recommended by MSB (2017) and have been used in other studies investigating pluvial flooding (Krvavica & Rubinić 2020; Y. Qiu et al. 2021).

For watercourses included as sources in the model, an adjustment was done to the available modelled discharge from S-HYPE for the relevant days, subtracting the mean discharge to correct for the watercourse surface already being included in the model. The surface was assumed to be the surface of a mean discharge, since there was no available information on when the scanning for the elevation model was done and the discharge at that time. This is of course an uncertain assumption that could lead to both an overestimation or underestimation of the discharge in the watercourses. This was another of the simplifications made of the model input, and an alternative way to do this would be to make a lowering in the elevation model to get the bare channel and then add the discharge without subtracting the mean discharge. This could be a more accurate way to describe the watercourses, but would demand additional information about their geometry and introduce another error since the watercourses would start as empty, overestimating their capacity to receive water without being flooded. Therefore the simpler method, with the unadjusted elevation model, was chosen, which is also regarded as generally being accurate enough by MSB (2014).

The effect of the uncertainties or simplifications of the model input will generally affect

how well the model represent the reality and might be seen in the comparison of the result from the spatially varied rain with validation data. But since the same input, apart from the precipitation, is applied in all scenarios, comparison between the results from the scenarios should not be highly affected by simplifications made in this.

5.3 Validation of the model results

With an aim to validate the model and get an estimation of how well it performs, the simulated results were compared with data from the flooding after the Gävle cloudburst. There were no official measurements of flooding depths or extent of flooded area available, so data points to use for validation had to be found individually and have different quality. Data point 1 is based on measurement by the owner on the facade of a house affected by the flooding where a mark could be seen where the water reached at it's highest level, which is probably a rather accurate estimation of the maximum flooding depth there. Several data points, 3, 4 and 5, are based on photos from the flooding, where the water level is seen to be reaching a point that can be identified in the elevation model, giving an estimation of the water depths in nearby depressions. In these cases simulated water depth at the time when the photo was taken is compared with the estimated real water depth. The estimations of the water level from photos are generally more uncertain than a measurement, even if they give an approximate value of the flooding depth at these places at the time of the photographing. Data point 2 is however based on both a photo of the water reaching up to a window and a measurement of the height of this window, this data point is estimated to be a rather accurate estimation of the flooding depth at this point when the photo was taken. An uncertainty of the estimations based on photos is that information of when the photo was taken often is based on the clock from a camera, which might not in all cases be updated to Swedish summer time or be completely accurate. Validation point 6 is only based on an observation of the water reaching up to a certain point which then is, in combination with the elevation model, giving a water depth in a nearby depression. This is not as precise as a photo of the water reaching up to this level, which is why the estimated real depth is presented as a range. The estimated real depth for validation point 7 is also estimated as a range since it is based on two photos of the water reaching almost up to the knees on two women. These are assumed to be of average height and the depth where estimated after measurements on calves, but is presented as a range due to the uncertainty.

The validation data could definitely have been more precise and numerous, but comparison with the data available shows that the model give a rather good estimation of the actual flooding depth after the cloudburst in Gävle. The results presented in Table 5 shows a difference of 1-4%, between the simulated response from the spatially varied rain and the actual response for point 1-5, which are assumed to be more accurate, with an average difference of 2.7% for these points. These results indicates that this model and the precipitation input based on 2×2 km radar data is accurate enough to describe the hydraulic response of the rain event with 96% accuracy. Comparison with validation point 6 and 7 gives an accuracy in the results of 88-100% and 57-100% respectively, which is rather large ranges and therefore is hard to evaluate the model with, but give an indication that it is not entirely wrong in these places. The validation data available did not give any indication that the spatially varied rain produced a lower flooding depth than the real rain event due to the averaging of rain intensity in the radar cells of 4 km^2 that the spatially varied rain is based on. To be able to conclude this, and that the rain represented the reality well, more surely the validation would preferably have been done with direct measurements of

the flooding depth and a larger number of validation points.

The validation indicates that the model with the spatially varied rains represents the actual cloudburst fairly well, however it does not give a strong indication that it represents the cloudburst better than the uniform rains. The flooding depth from the uniform rain with a mean hyetograph have an average difference from the actual flooding depth of 4.2% and the flooding from the uniform CDS rain differs by 3.7% from the actual. This is more than the 2.7% from the spatially varied, but the difference is small. Logically the spatially varied rain based on radar data from the event should generate a simulated flooding depth closer to the real one compared to uniform rains, but with the validation points available this conclusion could not be drawn surely. The rains will hereafter be discussed in relation to each other in terms of over- and underestimation. It is important however to keep in mind that an underestimation of a uniform rain compared to the spatially varied rain can not be interpreted as an underestimation compared to the actual rain event according to this validation, even though it possibly is the case.

Making a validation with crowdsourced data have been used as a solution in other cases were a real flooding event have been studied and direct measurements are lacking (Annis & Nardi 2019; Francipane et al. 2021; Mazzoleni et al. 2018). The large availability of cameras in the population is creating a great amount of photos, especially in extreme events, which is increasing the chance that some pictures are useful for validation. To use crowdsourced data is creating a chance for making validations or calibrations that otherwise would not have been available but it also has a risk with varying quality, and demand a lot of time for collecting and quality checking. Official measurements would have been preferable and a routine of measuring flooding depths after cloudbursts is recommended since this would enable better model validation and development, which in the long-term could prevent damages from flooding.

5.4 The influence of spatial variation on the hydraulic response

The results in this study points towards a significant difference between the hydraulic response in the model area from the spatially varied and uniform rain of a similar temporal variation and Figure 9 gives an overview of the difference in maximum flooding depth between the two rains. The uniform rain consists of the spatially averaged hyetograph from all the hyetographs connecting to the model area in the varied rain, which means it has the same total volume seen over the whole model and a similar temporal variation, isolating the factor of spatial variation in intensity. The figure shows clearly that there is a difference in maximum flooding depth using a uniform rain compared to a varied one. In this case the uniform rain underestimates the maximum flooding depths in the central part of the city by 5-35% in most streets (Figure 10) and in other parts of the model the flooding depth is instead slightly overestimated compared to the spatially varied rain. Hence the spatially varied rain was less intense in these parts than the average of the model area, while it in the central parts of the city was more intense than average, which can also be confirmed by studying the maximum rain intensity of the different radar cells in Figure 5a. Evaluating the statistics for the central parts of the model area, which is the area where the model is counted as valid due to a higher resolution, the uniform rain with a mean hyetograph is seen to have both smaller proportion of flooded area (-6%) and lower average maximum flooding depth (-6%) compared to the spatially varied rain (Table 7).

The relative difference from the maximum flooding depth of the spatially varied rain can become rather large compared to the absolute difference if the flooding depth is low. The relative difference might for example be 100%, but the absolute difference is only 1 cm in an area with a maximum flooding depth of 1 cm, and this difference is not important since the effect of this flooding is very small. Figure 11 shows the relative difference in flooding depth as previous figures, but only for the central parts of the area being counted as flooded by the spatially varied rain, i.e. reaching a maximum flooding depth of at least 0.1 m. These are the most interesting areas since it is were flooding occurs in the central parts of the model area that a difference in flooding depth can have a large effect. It is also in the central areas the model uses a higher resolution and can produce valid results. The results show that in most of the areas being flooded in the central part of the model the uniform rain is underestimating the flooding depth by 5-35% (Figure 11), and this underestimation is on average by 12% (Table 8). This means that even if Gävle municipality prepared by mapping the effect of a rain of this high intensity and with the right temporal variation, it would by using the common practise of uniform design storms have underestimated the effect of this rain in most of the central parts of the city, if assuming that the spatially varied rain represents the real rain. The results shows only the effect of the spatial variation in this specific case, where the more intense parts of the rain were centered over central parts of the city and might not be generally applicable to other cities or other rain events. But the results points out that a risk with using uniform design storms is a possible underestimation of the effect of a rain with a certain total volume or return period compared to using a spatially varied design storm, and presumably then also an underestimation of the effect compared to a real rain event. Studying the absolute difference in flooding depth in cm (Figure 12) the uniform rain is seen to give a up to over 15 cm lower flooding depth, but more commonly a difference of 3-15 cm in flooding depth where the difference is significant. This difference can be of importance but is probably not devastating, it does however point out a possible underestimation that should be further investigated. Spatial variations in intense rains can make a large part of the studied volume end up in smaller parts of a city, which in the worst case scenario is a sensitive part.

The results, that a spatially variable precipitation has a significant impact on the hydraulic response is well in line with studies presented in section 2.5. More specifically, the results showing that a spatially varied input increases the hydraulic response compared to a spatially uniform one, is also in agreement with other studies. Zhou et al. (2021) investigated the response in the form of flood peaks at urban watershed outlets of different spatially varied and uniform precipitation input and concluded that spatial varied input generally produced a higher flood peak, and that the difference became more pronounced for events of larger volume. The median flood peak was in the is study 22% higher using a spatially varied precipitation (Zhou et al. 2021). Similar findings were made by Zhu et al. (2018) in a more rural and larger study area, having the highest simulated flood peaks with the highest spatial resolution of the precipitation input, which was a 4 km^2 input as in the study of the Gävle cloudburst. Y. Qiu et al. (2021) compared simulated flood peaks of spatially varied and uniform rainfall input for 3 rain events and found that the spatially varied rainfall gave a higher simulated peak flow in 2 of the 3 events, with the largest difference for the most intense event where the spatially varied rain gave a 17.6% higher flow. The spatially varied rain was according to the validation performed in that study closer to the actual hydraulic response and was assessed to represent the reality well. In

the context of these case studies, carried out in catchments in the Midwestern US, Northeastern US and France there are indications that the results showing that a spatially varied rainfall input generates a higher hydraulic response than a uniform one are more general, and not only valid for this specific cloudburst in Gävle, and an indication that this should be taken into account when performing cloudburst modelling.

5.5 The influence of using CDS temporal variation on the hydraulic response

Common practice in cloudburst modelling and mapping is not only to use uniform design storms but also specifically to use uniform Chicago Design Storms, with the characteristic temporal variation in intensity they have, which is explained more closely in section 2.4.3. The CDS have a very pointy hyetograph, with a peak in the rain intensity which might be unrealistically high. This should generally overestimate the hydraulic response, since a large part of the total rain volume is falling during a short amount of time, producing overland flows when the water do not have time to infiltrate in the ground.

The CDS rain do have a higher peak than the real Gävle cloudburst (Figure 6), and the results show that it is giving a larger proportion of the area flooded compared to the spatially varied rain (+4%) and uniform rain with the mean hyetograph (+10%), even though they have the same total volume (Table 7). Comparing the uniform CDS with the uniform mean hyetograph rain isolates the factor of the temporal variation in rain intensity, since both these rains are spatially uniform and have the same total rain volume. The CDS rain gives an increase of the part of the area that is flooded by almost 10%, and a 3% higher average maximum flooding depth in the model compared to the uniform mean hyetograph rain (Table 7). These results tells us that in the Gävle cloudburst case the CDS temporal variation seems to make a general overestimation of the flooded area and average flooding depth compared to the mean hyetograph from the actual rain event. However a comparison with only one real event is not enough to draw conclusions about if CDS temporal variations in general make an overestimation of flooded area and flooding depth since an event with a different time to peak and general shape of the hyetograph could perform rather different in comparison with the CDS rain. The ratio of the time to peak and rainfall duration is concluded to increase the hydraulic response in a study by Mazurkiewicz & Skotnicki (2018), i.e. a peak occurring later in the rainfall event generates higher response. In the Gävle case however the peak in the CDS hyetograph occurs before the peak of the average hyetograph from the real event, and it is rather the pointiness of the CDS that is assumed to generate the higher hydraulic response.

Krvavica & Rubinić (2020) investigated and compared six different design storms for flood prediction and compared them with two historical events. Design storms based on Intensity-Duration-Frequency(IDF) curves, which is a group of design storms that CDS belongs to, was found to overestimate the flooding compared to historical events, while design storms based on observed temporal variations slightly underestimated or matched the flooding. This could imply that IDF-based design storms in general have higher peaks than actual cloudbursts and therefore generate a greater flooding depth.

Comparing the response from the uniform CDS rain with that from the uniform mean hyetograph is interesting since it investigates the effect of the temporal variation exclusively. However, comparing the uniform CDS with the spatially varied rain is more in-

teresting to investigate if the common practise of using uniform CDS design storms is reasonable, if assuming the spatially varied rain to represent the real rain event. The overestimation introduced by the CDS temporal variation compared to a real hyetograph could be argued to compensate for the underestimation introduced by using a uniform rainfall input compared to a spatially varied one, discussed in section 5.4, and thus be justified. The average maximum flooding depth is for example a bit lower using the uniform CDS rain, while it generates a larger part of the area counted as flooded (Table 7) compared to spatially varied rain. But although a general overestimation is done on the part of area that becomes flooded and the average maximum depth is only underestimated by 3% in comparison with the spatially varied rain, a larger underestimation and overestimation of flooding depth is still done in specific parts of the model area by using the uniform CDS rain. This can be seen in Figure 13 where the difference in flooding depth varies a lot between rather large both positive and negative values. More interestingly, when looking at only the central parts of the model area being flooded by the spatially varied rain (Figure 15), the CDS is seen to generally underestimate the flooding depth in the flooded parts, by 15-35% in many areas compared to the spatially varied rain. There are also within this area smaller parts that are overestimated as well, producing a general underestimation of 9%. This average difference is smaller compared to the flooding depth difference between the the spatially varied and the uniform mean hyetograph rain for the same area (-12%), but studying the figures showing the difference in flooding depths for the flooded central parts (Figure 11 and 15), and the average absolute value of the difference (Table 8), the uniform CDS rain can be seen to vary more, producing areas with higher both under- and overestimation of flooding depths. To be remembered is that all these are relative values which puts a higher weight on flooding depth differences where the flooding depth is low, since the relative difference than becomes larger. This is why the flooded parts (reaching water depth over 0.1 m) are analysed separately, but it can also be useful to look at the absolute flooding depth difference (Figure 16) which in this case shows a difference of up to 15 cm and on specific places over 15 cm between the uniform CDS rain and spatially varied. The variation between positive and negative difference can be seen here as well.

In conclusion, using a uniform CDS, which is commonly done in cloudburst modelling, could according to this study both generally overestimate the results due to the temporal variation compared to a real hyetograph rain and in some places underestimate the results due to the lack of spatial variation compared to a spatially varied rain, which means that the results have a considerable uncertainty in relation to a spatially varied rain with a real hyetograph and should be interpreted with this in mind. The calculation of the spatial average of the absolute values of the difference in the central and flooded area was an attempt to quantify this uncertainty in the parts that are of the highest interest and validity. The average difference was calculated to 15.7%, which can be interpreted as the uniform CDS rain is having an 15.7% uncertainty in flooding depths in this case, if the model with the spatially varied rain is assumed to generate the true flooding depths. This is higher than for the uniform rain with a mean hyetograph which had an average difference, or uncertainty, of 10.9% which indicates that using a CDS temporal variation introduces a further uncertainty compared to using the temporal variation of the actual rain event. It could be interpreted as the lack of spatial variation introducing an uncertainty of 10.9% and the CDS temporal variation increase this uncertainty further to 15.7% in this specific case and with the assumption that the spatially varied rain represents the real rain event.

These are results specific for this rain event and no investigation of the applicability to other places or rain events is done in this study. However the results are indicating that a risk of presenting a cloudburst mapping based on the assumptions of a uniform rain with a CDS temporal variation is that the results to broader public might be interpreted as the truth of what will happen if an extreme rainfall hits the area, and that the risk of a more severe flooding in parts of the area might be overlooked. The use of a uniform CDS seems, according to this study, to introduce an uncertainty in the result compared to a spatially varied rain and presumeably then also compared to the real rain, even if the validation in this case is to weak to confirm this. This possible uncertainty will be different for different rain events and places and deeper knowledge of the general uncertainties related to the cloudburst mapping based on uniform CDS rainfall is important and should be further investigated since this can effect how large safety margins are taken in relation to modelled results. Further studies comparing a spatially varied rainfall input with a uniform CDS one is therefore recommended, with a more extensive validation to be able to more surely conclude if a spatially varied rain represents a real rain event better than uniform scenarios, and to quantify the possible uncertainty introduced by using uniform CDS rains for different places and events which could lead to general conclusions about this.

6 CONCLUSIONS

The influence of spatial variation of rainfall intensity was investigated by comparing simulated hydraulic response in a model from spatially varied and uniform rainfall input based on the cloudburst event in Gävle on the 17-18 of August 2021. Evaluation was done for the central part of the model area, which has the highest validity due to higher resolution and is of higher interest since flooding in this area generally causes greater damage and affects more people. Comparison with 7 validation data points within this central part is done and the simulated flooding depths from the spatially varied rain were generally consistent with these, indicating that it represents the actual cloudburst well. However the validation could not confirm that the spatially varied rain represents the actual rain event better than the uniform ones, and a more extensive validation is needed to draw conclusions about this.

A spatially uniform design storm with the same temporal variation in rain intensity, isolating the factor of spatial variation, was shown to give a lower average maximum flooding depth and smaller proportion of the area flooded in the central part of the model area compared to the spatially varied rain. Mapping of the flooding depth difference between the two rains in the central parts of the area showed that the flooded areas in most of the city was underestimated by 5-35% in this case, with an average underestimation of 9% by the uniform rain compared to the varied. This lead to a conclusion that simulating a rain as spatially uniform can lead to a general underestimation of the flooding depth and in specific parts of the model lead to a more pronounced underestimation, compared to a spatially varied rainfall input.

A spatially uniform design storm with a CDS temporal variation, which is what is commonly used in cloudburst modelling today, was shown to give a slightly lower average maximum flooding depth but a larger proportion of the area being flooded in comparison

to the spatially varied rain in the central part of the model. Mapping of the flooding depth difference showed that it was highly varying throughout the model area but in central and flooded parts the flooding depth was generally underestimated by the uniform CDS compared to the spatially varied rain. The results of a varying flooding depth difference indicates that using a uniform CDS introduces an uncertainty in the results in relation to the varied rain, since it can both under- and overestimate the flooding depth. This uncertainty or variation was quantified as 15.7% in the central and flooded area in this case.

The difference in hydraulic response identified in the use of a uniform design storm, and specifically and more enhanced, a uniform CDS in cloudburst modelling compared to a spatially varied rain with a real temporal variation is an important conclusion from this study. Further studies are recommended with a more extensive validation to determine how well a spatially varied rain represents the reality and to quantify the difference in hydraulic response between a spatially varied rain and uniform CDS for different places and rain events. This could give important information about the possible uncertainties in cloudburst mapping based on a uniform CDS, which should be included in a comprehensible way when results are presented, so the right safety margins are used when societal decisions are based on these results.

REFERENCES

Annis, A. & Nardi, F. (Oct. 2019). Integrating VGI and 2D hydraulic models into a data assimilation framework for real time flood forecasting and mapping. *Geo-spatial Information Science*, vol. 22 (4), p. 223–236. Available: https://doi.org/10.1080/10095020.2019.1626135 [01/27/2022].

Arnell, V. (1982). "Rainfall Data for the Design of Sewer Pipe Systems". en. Dissertation. PhD thesis. Chalmers tekniska högskola. Available: https://research.chalmers.se/en/publication/167236 [09/24/2021].

Bell, V. A. & Moore, R. J. (Jan. 2000). The sensitivity of catchment runoff models to rainfall data at different spatial scales. en. *Hydrology and Earth System Sciences*, vol. 4 (4). Publisher: Copernicus Publications, p. 653–667. Available: http://www.hydrol-earth-syst-sci.net/4/653/2000/hess-4-653-2000.pdf [09/08/2021].

Bengtsson, O. (Sept. 2021). Skador för en halv miljard efter skyfallen i Gävle och Dalarna. sv. *SVT Nyheter*. Available: https://www.svt.se/nyheter/inrikes/skador-for-en-halv-miljard-efter-skyfallen-i-gavle-och-dalarna [12/22/2021].

Brath, A., Montanari, A., & Toth, E. (June 2004). Analysis of the effects of different scenarios of historical data availability on the calibration of a spatially-distributed hydrological model. en. *Journal of Hydrology*. Catchment modelling: Towards an improved representation of the hydrological processes in real-world model applications, vol. 291 (3), p. 232–253. DOI: 10.1016/j.jhydrol.2003.12.044. Available: https://www.sciencedirect.com/science/article/pii/S0022169404000344 [09/27/2021].

Carpman, A. (Aug. 2018). Sterilcentralen åter i drift på Akademiska. sv. *Dagens Medicin*. Available: https://www.dagensmedicin.se/alla-nyheter/nyheter/sterilcentralen-ater-i-drift-pa-akademiska/ [09/17/2021].

Dahlström, B. (2010). *Regnintensitet – en molnfysikalisk betraktelse*. sv. Tech. rep., p. 46.

DHI (2017). *MIKE 21 Flow Model FM Hydrodynamic Module- User Guide*. Tech. rep. Available: https://manuals.mikepoweredbydhi.help/2017/Coast_and_Sea/MIKE_FM_HD_2D.pdf [12/02/2021].

DHI (2020a). *MIKE 21 Flow Model Hydrodynamic Module- User Guide*. Tech. rep. Available: https://manuals.mikepoweredbydhi.help/2020/MIKE_21.htm [09/16/2021].

DHI (2020b). *MIKE Zero, The Common DHI User Interface for Project Oriented Water Modelling - User Guide*. Tech. rep. Available: https://manuals.mikepoweredbydhi.help/2020/General/MIKEZero.pdf.

Elfström, D. & Stefansson, M. (2021). "How design storms with normally distributed intensities customized from precipitation radar data in Sweden affect the modeled hydraulic response to extreme rainfalls". eng. MA thesis. Uppsala University. Available: http://urn.kb.se/resolve?urn=urn:nbn:se:uu:diva-437729 [03/15/2022].

Faurès, J.-M., Goodrich, D. C., Woolhiser, D. A., & Sorooshian, S. (Dec. 1995). Impact of small-scale spatial rainfall variability on runoff modeling. en. *Journal of Hydrology*, vol. 173 (1), p. 309–326. DOI: 10.1016/0022-1694(95)02704-S. Available: https://www.sciencedirect.com/science/article/pii/002216949502704S [09/08/2021].

Fiener, P. & Auerswald, K. (2009). Spatial variability of rainfall on a sub-kilometre scale. en. *Earth Surface Processes and Landforms*, vol. 34 (6), p. 848–859. DOI: 10.1002/esp.1779. Available: http://onlinelibrary.wiley.com/doi/abs/10.1002/esp.1779 [09/09/2021].

Forsell, D. (July 2018). Regnrekord i Uppsala – "Ovanligt med så mycket regn på så kort tid". sv. *SVT Nyheter*. Available: https://www.svt.se/nyheter/lokalt/uppsala/kraftiga-regnet-i-uppsala-ovanligt-med-sa-mycket-regn-pa-sa-kort-tid [09/17/2021].

Francipane, A., Pumo, D., Sinagra, M., La Loggia, G., & Noto, L. V. (Aug. 2021). A paradigm of extreme rainfall pluvial floods in complex urban areas: the flood event of 15 July 2020 in Palermo (Italy). en. *Natural Hazards and Earth System Sciences*, vol. 21 (8), p. 2563–2580. DOI: 10.5194/nhess-21-2563-2021. Available: https://nhess.copernicus.org/articles/21/2563/2021/ [01/26/2022].

Goodrich, D. C., Faurès, J.-M., Woolhiser, D. A., Lane, L. J., & Sorooshian, S. (Dec. 1995). Measurement and analysis of small-scale convective storm rainfall variability. en. *Journal of Hydrology*, vol. 173 (1), p. 283–308. DOI: 10.1016/0022-1694(95)02703-R. Available: https://www.sciencedirect.com/science/article/pii/002216949502703R [09/08/2021].

Goudenhoofdt, E. & Delobbe, L. (Feb. 2009). Evaluation of radar-gauge merging methods for quantitative precipitation estimates. en. *Hydrology and Earth System Sciences*, vol. 13 (2). Publisher: Copernicus Publications, p. 195–203. Available: http://www.hydrol-earth-syst-sci.net/13/195/2009/hess-13-195-2009.pdf [10/07/2021].

Grip, H. & Rodhe, A. (2016). *Vattnets väg från regn till bäck*. swe. Uppsala universitet. Available: http://urn.kb.se/resolve?urn=urn:nbn:se:uu:diva-307562 [09/23/2021].

Hanchoowong, R., Weesakul, U., & Chumchean, S. (Dec. 2012). Bias correction of radar rainfall estimates based on a geostatistical technique. *ScienceAsia*, vol. 38, p. 373. DOI: 10.2306/scienceasia1513-1874.2012.38.373.

Hendriks, M. R. (2010). *Introduction to physical hydrology*. English. Book, Whole. New York;Oxford; Oxford University Press. Available: https://go.exlibris.link/wG6rVnsF [09/15/2021].

Hernebring, C., Milotti, S., Steen Kronborg, S., Wolf, T., & Mårtensson, E. (2015). The cloudburst in Southwestern Scania 2014-08-31 With focus on consequences and in relation to rainfall statistics in Malmö. Available: https://www.tidskriftenvatten.se/tsv-artikel/skyfallet-i-sydvastra-skane-2014-08-31-fokuserat-mot-konsekvenser-och-relation-till-regnstatistik-i-malmo-the-cloudburst-in-southwestern-scania-2014-08-31-with-focus-on-consequences-and-in-relation/ [08/31/2021].

IPCC (2021). "Summary for Policymakers". *Climate Change 2021: The Physical Science Basis. Contribution of Working Group I to the Sixth Assessment Report of the Intergovernmental Panel on Climate Change*. Ed. by V. Masson-Delmotte, P. Zhai, A. Pirani, S. Connors, C. Péan, S. Berger, N. Caud, E. Chen, L. Goldfarb, M. Gomis, J. Huang, K. Leitzell, Lonnoy, J. Matthews, T. Maycock, T. Waterfield, O. Yelekci, R. Yu, & B. Zhou. Section: SPM Type: Book Section. Cambridge, United Kingdom and New York, NY, USA: Cambridge University Press, p. 1–30. DOI: 10.1017/CBO9781107415324.004. Available: www.climatechange2013.org.

Kaspersen, P. S., Ravn, N. H., Arnbjerg-Nielsen, K., Madsen, H., & Drews, M. (Aug. 2017). Comparison of the impacts of urban development and climate change on exposing European cities to pluvial flooding. en. *Hydrology and Earth System Sciences*, vol. 21. Publisher: Copernicus Publications, p. 4131–4147. DOI: 10.5194/hess-21-4131-2017. Available: https://www.hydrol-earth-syst-sci.net/21/4131/2017/hess-21-4131-2017.pdf [09/07/2021].

Keifer, C. J. & Chu, H. H. (1957). Synthetic Storm Pattern for Drainage Design. eng. *Journal of the Hydraulics Division*, vol. 83 (4). Publisher: ASCE, p. 1–25. Available: https://cedb.asce.org/CEDBsearch/record.jsp?dockey=0010917 [09/23/2021].

Krajewski, W. F., Lakshmi, V., Georgakakos, K. P., & Jain, S. C. (1991). A Monte Carlo Study of rainfall sampling effect on a distributed catchment model. en. *Water Resources Research*, vol. 27 (1), p. 119–128. DOI: 10.1029/90WR01977. Available: http://onlinelibrary.wiley.com/doi/abs/10.1029/90WR01977 [09/27/2021].

Krvavica, N. & Rubinić, J. (July 2020). Evaluation of Design Storms and Critical Rainfall Durations for Flood Prediction in Partially Urbanized Catchments. en. *Water*, vol. 12 (2044). Publisher: MDPI AG, p. 2044. DOI: 10.3390/w12072044. Available: https://www.mdpi.com/2073-4441/12/7/2044 [02/09/2022].

Maier, R., Krebs, G., Pichler, M., Muschalla, D., & Gruber, G. (Apr. 2020). Spatial Rainfall Variability in Urban Environments—High-Density Precipitation Measurements on a City-Scale. en. *Water*, vol. 12 (1157). Publisher: MDPI AG, p. 1157. DOI: 10.3390/w12041157. Available: https://www.mdpi.com/2073-4441/12/4/1157 [09/02/2021].

Mazurkiewicz, K. & Skotnicki, M. (Jan. 2018). The influence of synthetic hyetograph parameters on simulation results of runoff from urban catchment. *E3S Web of Conferences*, vol. 30, p. 01018. DOI: 10.1051/e3sconf/20183001018.

Mazzoleni, M., Cortes, J., Wehn, U., Alfonso, L., Norbiato, D., Monego, M., Ferri, M., & Solomatine, D. (Jan. 2018). Exploring the influence of citizen involvement on the assimilation of crowdsourced observations: A modelling study based on the 2013 flood event in the Bacchiglione catchment (Italy). *Hydrology and Earth System Sciences*, vol. 33, p. 391–416. DOI: 10.5194/hess-22-391-2018.

McKee, J. L. & Binns, A. D. (2016). A review of gauge-radar merging methods for quantitative precipitation estimation in hydrology. English. *Canadian water resources journal*, vol. 41 (1-2). ISBN: 0701-1784, p. 186–203.

McKee, J. L., Binns, A. D., Helsten, M., & Shifflett, M. (2018). Evaluation of Gauge-Radar Merging Methods Using a Semi-Distributed Hydrological Model in the Upper Thames River Basin, Canada. en. *JAWRA Journal of the American Water Resources Association*, vol. 54 (3), p. 594–612. DOI: 10.1111/1752-1688.12625. Available: http://onlinelibrary.wiley.com/doi/abs/10.1111/1752-1688.12625 [10/07/2021].

MSB (2012). *Översvämningar i Sverige 1901-2010.* sv. Tech. rep. OCLC: 940289820. Karlstad: Myndigheten för samhällsskydd och beredskap (MSB).

MSB (2013). *Pluviala översvämningar : konsekvenser vid skyfall över tätorter, en kunskapsöversikt*. sv. Tech. rep. MSB567-13, p. 70. Available: https://www.msb.se/RibData/Filer/pdf/26609.pdf.

MSB (2014). *Kartläggnign av skyfalls påverkan på samhällsviktig verksamhet- framtagande av metodik för utredning på kommunal nivå*. sv. Tech. rep. MSB694, p. 64. Available: https://rib.msb.se/filer/pdf/27365.pdf.

MSB (2017). *Vägledning för skyfallskartering: tips för genoförande och exempel på användning*. sv. OCLC: 1023376598. Karlstad: Myndigheten för samhällsskydd och beredskap (MSB).

Niemczynowicz, J. (1984). "An investigation of the areal and dynamic properties of rainfall and its influence of runoff-generating processes". English. Volume: 1005 Dissertation/Thesis. PhD thesis. Lund. Available: https://go.exlibris.link/qKX5hbGX [09/23/2021].

Ochoa-Rodriguez, S., Wang, L.-P., Willems, P., & Onof, C. (2019). A Review of Radar-Rain Gauge Data Merging Methods and Their Potential for Urban Hydrological Applications. en. *Water Resources Research*, vol. 55 (8), p. 6356–6391. DOI: 10.1029/2018WR023332. Available: http://onlinelibrary.wiley.com/doi/abs/10.1029/2018WR023332 [10/04/2021].

Ochoa-Rodriguez, S., Wang, L.-P., Gires, A., Pina, R. D., Reinoso-Rondinel, R., Bruni, G., Ichiba, A., Gaitan, S., Cristiano, E., Assel, J. van, Kroll, S., Murlà-Tuyls, D., Tisserand, B., Schertzer, D., Tchiguirinskaia, I., Onof, C., Willems, P., & Veldhuis, M.-C. ten (Dec. 2015). Impact of spatial and temporal resolution of rainfall inputs on urban hydrodynamic modelling outputs: A multi-catchment investigation. en. *Journal of Hydrology*. Hydrologic Applications of Weather Radar, vol. 531, p. 389–407. DOI: 10.1016/j.jhydrol.2015.05.035. Available: https://www.sciencedirect.com/science/article/pii/S0022169415003856 [09/09/2021].

Olsson, J. (2019). "The influence of storm movement and temporal variability of rainfall on urban pluvial flooding : 1D-2D modelling with empirical hyetographs and CDS-rain". eng. MA thesis. Uppsala University. Available: http://urn.kb.se/resolve?urn=urn:nbn:se:uu:diva-387898 [09/13/2021].

Olsson, J., Berg, P., Eronn, A., Simonsson, L., Södling, J., Wern, L., & Yang, W. (2017). Extremregn i nuvarande och framtida klimat. sv, p. 83.

Peleg, N., Blumensaat, F., Molnar, P., Fatichi, S., & Burlando, P. (Mar. 2017). Partitioning the impacts of spatial and climatological rainfall variability in urban drainage modeling. en. *Hydrology and Earth System Sciences*, vol. 21 (3). Publisher: Copernicus Publications, p. 1559–1572. DOI: 10.5194/hess-21-1559-2017. Available: http://www.hydrol-earth-syst-sci.net/21/1559/2017/hess-21-1559-2017.pdf [09/08/2021].

Qiu, Q., Liu, J., Tian, J., Jiao, Y., Li, C., Wang, W., & Yu, F. (Jan. 2020). Evaluation of the Radar QPE and Rain Gauge Data Merging Methods in Northern China. en. *Remote Sensing*, vol. 12 (3). Number: 3 Publisher: Multidisciplinary Digital Publishing Institute, p. 363. DOI: 10.3390/rs12030363. Available: https://www.mdpi.com/2072-4292/12/3/363 [10/07/2021].

Qiu, Y., Paz, I. d. S. R., Chen, F., Versini, P.-A., Schertzer, D., & Tchiguirinskaia, I. (June 2021). Space variability impacts on hydrological responses of nature-based solutions and the resulting uncertainty: a case study of Guyancourt (France). en. *Hydrology and Earth System Sciences*, vol. 25. Publisher: Copernicus Publications, p. 3137–3162. DOI: 10.5194/hess-25-3137-2021. Available: https://hess.copernicus.org/articles/25/3137/2021/hess-25-3137-2021.pdf [02/02/2022].

Ritchie, H. & Roser, M. (June 2014). Natural Disasters. *Our World in Data*. Available: https://ourworldindata.org/natural-disasters [12/16/2021].

SCB (Aug. 2021). *Folkmängd i riket, län och kommuner 30 juni 2021 och befolkningsförändringar 1 april–30 juni 2021*. sv. Available: https://www.scb.se/hitta-statistik/statistik-efter-amne/befolkning/befolkningens-sammansattning/befolkningsstatistik/pong/tabell-och-diagram/kvartals--och-halvarsstatistik--kommun-lan-och-riket/kvartal-2-2021/ [10/13/2021].

Segond, M.-L., Wheater, H. S., & Onof, C. (Dec. 2007). The significance of spatial rainfall representation for flood runoff estimation: A numerical evaluation based on the Lee catchment, UK. en. *Journal of Hydrology*, vol. 347 (1), p. 116–131. DOI: 10.1016/j.jhydrol.2007.09.040. Available: https://www.sciencedirect.com/science/article/pii/S0022169407004933 [09/24/2021].

Skougaard Kaspersen, P., Høegh Ravn, N., Arnbjerg-Nielsen, K., Madsen, H., & Drews, M. (Aug. 2017). Comparison of the impacts of urban development and climate change on exposing European cities to pluvial flooding. English. *Hydrology and Earth System Sciences*, vol. 21 (8). Publisher: Copernicus GmbH, p. 4131–4147. DOI: 10.5194/hess-21-4131-2017. Available: https://hess.copernicus.org/articles/21/4131/2017/hess-21-4131-2017.html [11/26/2021].

SMHI (Feb. 2019). *Återkomsttider för extremt väder — SMHI*. Available: https://www.smhi.se/professionella-tjanster/professionella-tjanster/statistik-och-data/aterkomsttider-for-extremt-vader-1.14134 [09/10/2021].

SMHI (Sept. 2021a). *Augusti 2021 - Regnig månad med skyfall över Gävle — SMHI*. Available: https://www.smhi.se/klimat/klimatet-da-och-nu/manadens-vader-och-vatten-sverige/manadens-vader-i-sverige/augusti-2021-meteorologi-1.173428 [09/17/2021].

SMHI (Apr. 2021b). *Extremt väder — SMHI*. Available: https://www.smhi.se/kunskapsbanken/klimat/extremer/extremt-vader-1.5779 [09/10/2021].

SMHI (June 2021c). *Extrem nederbörd — SMHI*. Available: https://www.smhi.se/kunskapsbanken/meteorologi/extrem-nederbord-1.23060 [09/10/2021].

SMHI (Aug. 2021d). *Svenska nederbördsrekord — SMHI*. Available: https://www.smhi.se/kunskapsbanken/meteorologi/svenska-nederbordsrekord-1.6660 [09/17/2021].

SMHI (2021e). *Modelldata per område — SMHI - Vattenwebb*. Available: http://vattenwebb.smhi.se/modelarea/ [10/19/2021].

SMHI (2021f). *Ladda ner meteorologiska observationer — SMHI*. Available: https://www.smhi.se/data/meteorologi/ladda-ner-meteorologiska-observationer#param=precipitation15MinutesSum,stations=all [01/18/2022].

Smith, J. A., Baeck, M. L., Meierdiercks, K. L., Miller, A. J., & Krajewski, W. F. (Oct. 2007). Radar rainfall estimation for flash flood forecasting in small urban watersheds. en. *Advances in Water Resources*. Recent Developments in Hydrologic Analysis, vol. 30 (10), p. 2087–2097. DOI: 10.1016/j.advwatres.2006.09.007. Available: https://www.sciencedirect.com/science/article/pii/S0309170807000553 [10/12/2021].

Smith, J. A. & Krajewski, W. F. (1991). Estimation of the Mean Field Bias of Radar Rainfall Estimates. *Journal of Applied Meteorology (1988-2005)*, vol. 30 (4). Publisher: American Meteorological Society, p. 397–412. Available: http://www.jstor.org/stable/26185463 [10/18/2021].

Stull, R. (2017). *Practical Meteorology: An Algebra-based Survey of Atmospheric Science*. Univ. of British Columbia. Available: https://www.eoas.ubc.ca/books/Practical_Meteorology/.

Svenskt Vatten (2011). *Nederbördsdata vid dimensionering och analys av avloppssystem*. swe. 1. utgåvan. Publikation / Svenskt vatten 104. Stockholm: Svenskt vatten.

Svenskt Vatten (2016). *Avledning av dag-, drön- och spillvatten*. swe. 1. utgåvan. Publikation / Svenskt vatten 110. Stockholm: Svenskt vatten.

Svenskt Vatten (2020). *Nederbördsstatistik för dimensionering av dagvattensystem – State of the art*. sv-SE. Tech. rep. Available: https://vattenbokhandeln.svensktvatten.se/produkt/nederbordsstatistik-for-dimensionering-av-dagvattensystem-state-of-the-art/ [09/06/2021].

Thorndahl, S., Nielsen, J. E., & Rasmussen, M. R. (Jan. 2014). Bias adjustment and advection interpolation of long-term high resolution radar rainfall series. en. *Journal of Hydrology*, vol. 508, p. 214–226. DOI: 10.1016/j.jhydrol.2013.10.056. Available: https://www.sciencedirect.com/science/article/pii/S0022169413008160 [10/17/2021].

Wardhana, A., Pawitan, H., & Dasanto, B. D. (Mar. 2017). Application of hourly radar-gauge merging method for quantitative precipitation estimates. *IOP Conference Series: Earth and Environmental Science*, vol. 58. Publisher: IOP Publishing, p. 012033. DOI: 10.1088/1755-1315/58/1/012033. Available: https://doi.org/10.1088/1755-1315/58/1/012033.

Wright, D. B., Smith, J. A., Villarini, G., & Baeck, M. L. (2014). Long-Term High-Resolution Radar Rainfall Fields for Urban Hydrology. en. *JAWRA Journal of the American Water Resources Association*, vol. 50 (3), p. 713–734. DOI: 10.1111/jawr.12139. Available: http://onlinelibrary.wiley.com/doi/abs/10.1111/jawr.12139 [10/17/2021].

Vägverket (2008). *VVMB 310 Hydraulisk dimensionering*. 2008:61. Vägverket.

Xing, Y., Liang, Q., Wang, G., Ming, X., & Xia, X. (Mar. 2019). City-scale hydrodynamic modelling of urban flash floods: the issues of scale and resolution. en. *Natural Hazards*, vol. 96 (1). Company: Springer Distributor: Springer Institution: Springer Label: Springer Number: 1 Publisher: Springer Netherlands, p. 473–496. DOI: 10.1007/s11069-018-3553-z. Available: http://link.springer.com/article/10.1007/s11069-018-3553-z [02/02/2022].

Zhou, Z., Smith, J. A., Baeck, M. L., Wright, D. B., Smith, B. K., & Liu, S. (Aug. 2021). The impact of the spatiotemporal structure of rainfall on flood frequency over a small urban watershed: an approach coupling stochastic storm transposition and hydrologic modeling. en. *Hydrology and Earth System Sciences*, vol. 25. Publisher: Copernicus Publications, p. 4701–4717. DOI: 10.5194/hess-25-4701-2021. Available: https://hess.copernicus.org/articles/25/4701/2021/hess-25-4701-2021.pdf [01/25/2022].

Zhu, Z., Wright, D. B., & Yu, G. (2018). The Impact of Rainfall Space-Time Structure in Flood Frequency Analysis. en. *Water Resources Research*, vol. 54 (11), p. 8983–8998. DOI: 10.1029/2018WR023550. Available: http://onlinelibrary.wiley.com/doi/abs/10.1029/2018WR023550 [01/25/2022].

A APPENDIX

A.1 Correction of radar estimated data against measured data

```
%Import radar data
precip= ncread('gavle_20210817-20210818_15min.nc', 'pr');
time= ncread('gavle_20210817-20210818_15min.nc', 'time');
lat= ncread('gavle_20210817-20210818_15min.nc', 'lat');
lon= ncread('gavle_20210817-20210818_15min.nc', 'lon');

%The four radarcells in connection to the station
r1=squeeze(precip(23,19, :));
r2=squeeze(precip(23,18, :));
r3=squeeze(precip(24,19, :));
r4=squeeze(precip(24,18, :));

lat1= [60.7246 60.7161];
lon1= [17.1464 17.1607];
lat2= [60.7067 60.7161];
lon2= [17.1443 17.1607];
lat3= [60.7236 60.7161];
lon3= [17.1831 17.1607];
lat4= [60.7057 60.7161];
lon4= [17.1810 17.1607];

%Distance between the middle of the radar cells and the station
dist1=stdist(lat1, lon1);
dist2=stdist(lat2, lon2);
dist3=stdist(lat3, lon3);
dist4=stdist(lat4, lon4);

dist_tot=1/dist1+1/dist2+1/dist3+1/dist4;

%Creating factors with a higher value for shorter distance, adding up to 1
faktor1=(1/dist1/dist_tot)
faktor2=(1/dist2/dist_tot)
faktor3=(1/dist3/dist_tot)
faktor4=(1/dist4/dist_tot)


%Weighting of the data from teh four cells depending on the distance to the station
radar=zeros(192,1);
for i=1:length(time)
radar(i,1)=faktor1*r1(i,1)+ faktor2*r2(i,1)+ faktor3*r3(i,1)+faktor4*r4(i,1);
end

%Importing measurement from SMHI station and converting to mm/h
load Gavle20210902_121759.csv ; %data from station in mm/15 min
gavle= Gavle20210902_121759 ;
station= gavle(10938:11129,9).*4; %rain intensity [mm/h]

%Create vectors with the mean intensity per hour
r=1;
for i=1:length(radar)/4
radar2(i)= mean(radar(r:(r+3)));
r=r+4;
end
```

```
r=1;
for i=1:length(radar)/4
station2(i)= mean(station(r:(r+3)));
r=r+4;
end

%Creating correction factor series of the mean intensity per hour values
correction=ones(48,1).*mean(station(1:128))/mean(radar(1:128)); %average ratio-vector
z=find(station2 & radar2); %Find positions where both radar and station data are non-z
correction(z)=station2(z)./radar2(z);  %Find relation between hourly intensity values
correction(correction>4)=4;
correction_2=repelem(correction,4);  %Repeats every value 4 times to get a vector of t
%same length as original data

%Correcting radar data
corrected_radar= precip;
for i=1:192
corrected_radar(:,:,i)=correction_2(i)*precip(:,:,i);
end
```

A.2 Flooding statistics for the full model and the central area

Table A.1: Statistics of the hydraulic response from the simulation of the different rain scenarios in the full model area and in the central part of the model area

Rain scenario	**Part of area flooded**			
	Full model	Difference from spatial	Central part	Difference from spatial
Spatially varied	31.3%	-	27.6%	-
Uniform mean hyetograph	31.6%	+1%	26.1%	-6%
Uniform CDS hyetograph	33.7%	+7%	28.6%	+4%
Rain scenario	**Average maximum flooding depth**			
	Full model	Difference from spatial	Central part	Difference from spatial
Spatially varied	16.2 cm	-	12.5 cm	-
Uniform mean hyetograph	15.8 cm	-3%	11.7 cm	-6%
Uniform CDS hyetograph	16.2 cm	0%	12.1 cm	-3%

A.3 Maximum flooding depth for uniform scenarios

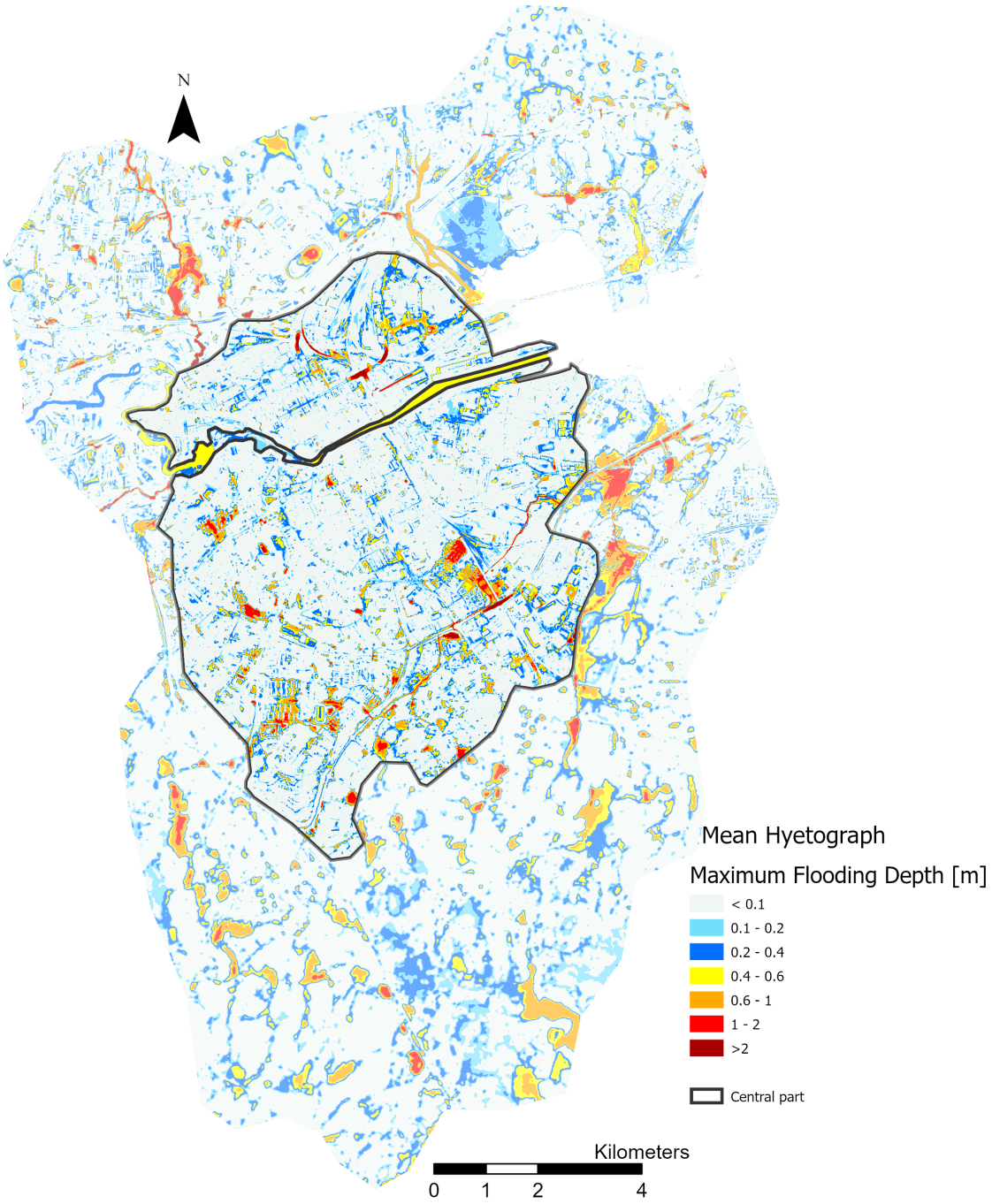

Figure A.1: The maximum flooding depth of the uniform rain with a mean hyetograph given in meters. The central part of the area is marked with a black outline.

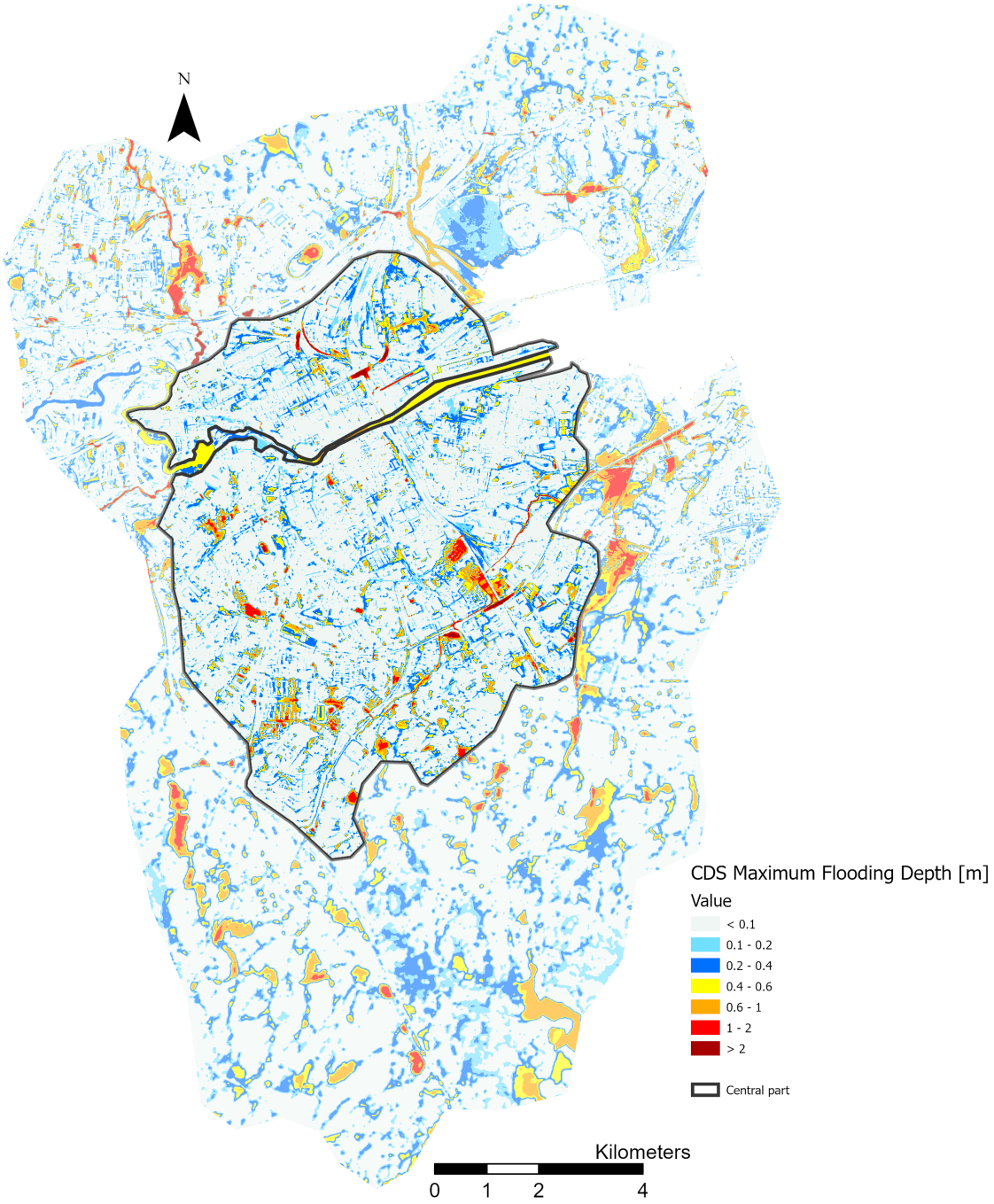

Figure A.2: The maximum flooding depth of the uniform CDS rain given in meters. The central part of the area is marked with a black outline.

A.4 Flooding depth difference in cm for uniform scenarios

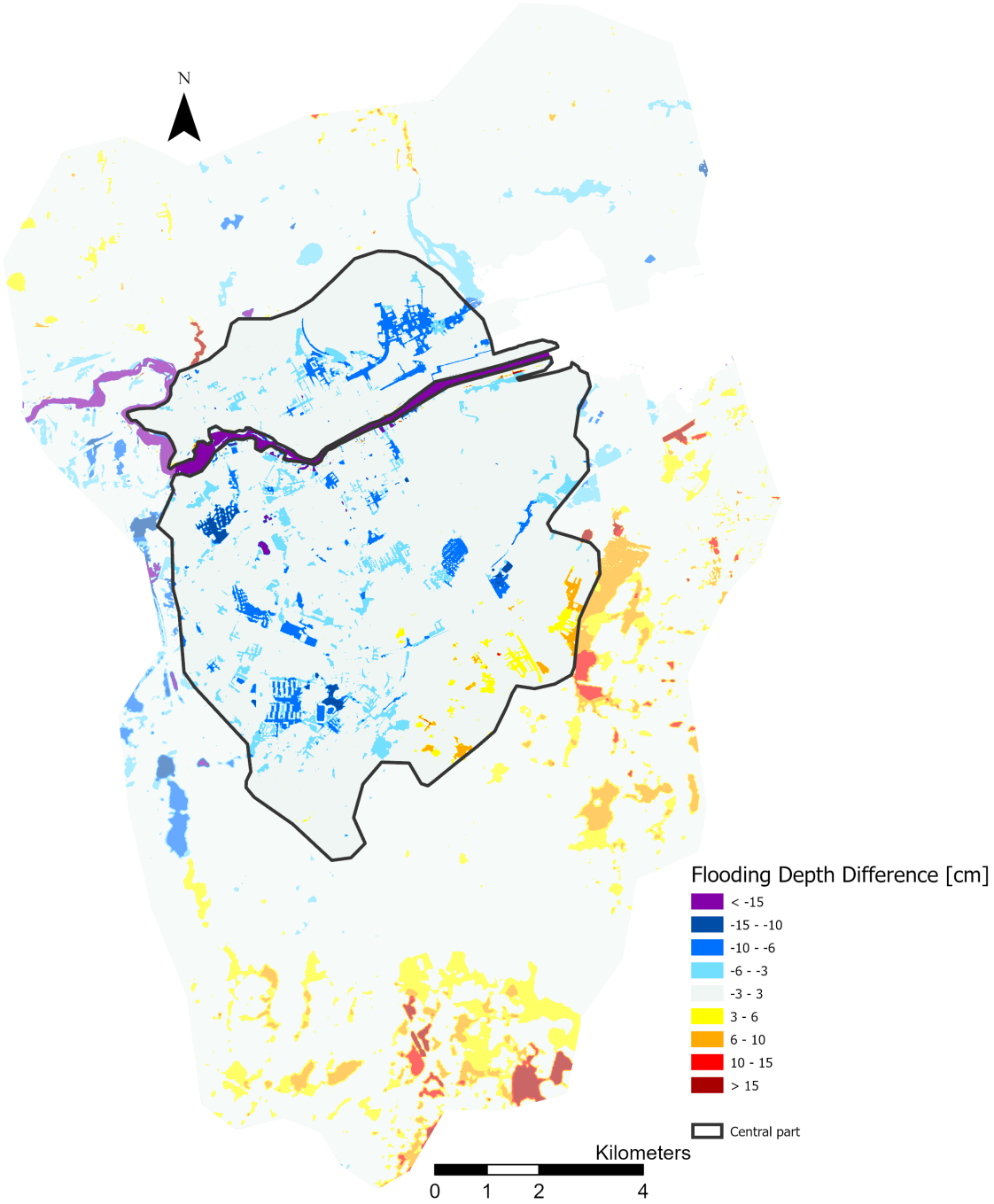

Figure A.3: The flooding depth difference between the uniform rain with a mean hyetograph and the spatially varied rain given in centimeters. Calculated by subtracting flooding depth by uniform rain from flooding depth by spatial rain.

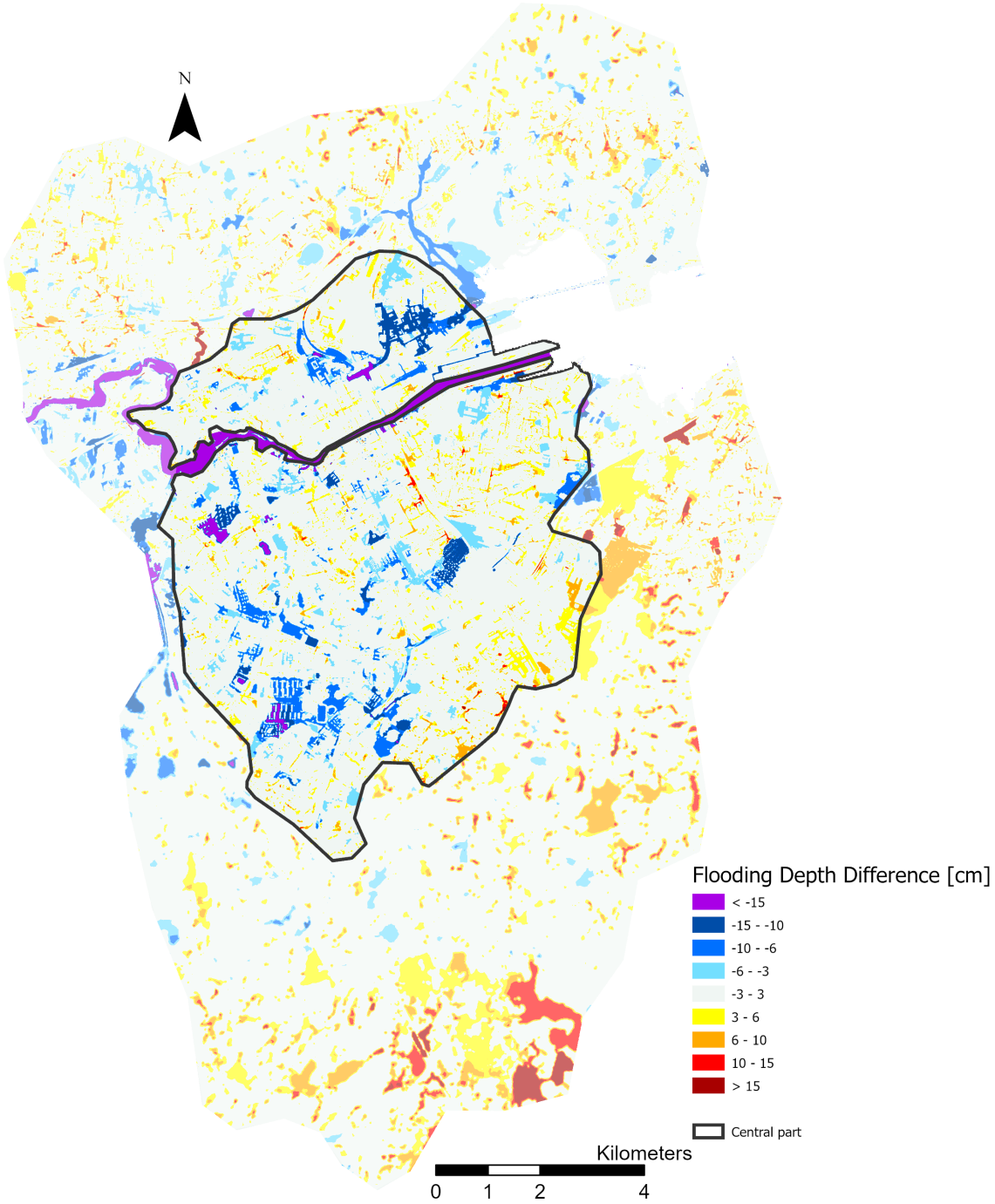

Figure A.4: The flooding depth difference between the uniform rain with a CDS hyetograph and the spatially varied rain given in centimeters. Calculated by subtracting flooding depth by uniform rain from flooding depth by spatial rain.